



T.C.

ALTINBAS UNIVERSITY

Institute of Graduate Studies

Mechanical Engineering

**MODIFYING A GENERATOR AND DESIGNING  
A SOLAR COLLECTOR**

Marwah AL-DAYYENI

Master of Science

Supervisor

Asst. Prof. Dr. Ibrahim KOÇ

**Istanbul, 2021**

# **MODIFYING A GENERATOR AND DESIGNING A SOLAR COLLECTOR**

By

Marwah Ali Hussien AL-DAYYENI

Mechanical Engineering

Submitted to the Graduate School of Science and Engineering  
in partial fulfillment of the requirements for the degree of  
Master of Science

ALTINBAŞ UNIVERSITY

2021

The thesis “MODIFYING A GENERATOR AND DESIGNING A SOLAR COLLECTOR” prepared and presented by Marwah AL-DAYYENI was accepted as a Master of science in Mechanical Engineering.

---

Asst. Prof. Dr. Ibrahim KOÇ

Supervisor

Thesis Defense Jury Members:

Asst. Prof. Ibrahim KOÇ      School of Engineering and  
Natural Sciences,  
Altinbas University

Asst. Prof. Serdar AY      School of Engineering and  
Natural Sciences,  
Altinbas University

Asst. Prof. Haydar UYANIK      School of Applied ,  
Sciences  
KTO Karatay Univerisity

I certify that this thesis satisfies all the requirements as a thesis for the degree of Master of Science.

Approval Date of Institute of Graduate Studies: \_\_\_\_/\_\_\_\_/\_\_\_\_

I hereby declare that all information in this document has been obtained and presented in accordance with academic rules and ethical conduct. I also declare that, as required by these rules and conduct, I have fully cited and referenced all material and results that are not original to this work.

Marwah Ali Hussien AL-DAYYENI

## DEDICATION

Praise be to God, and it is enough, and prayers be upon the beloved Mustafa, his family, and those who follow: Praise be to God, who has enabled us to value this step in my academic career with my memoir. This is the fruit of effort and success.

Man was found on the face of the earth, and he did not live in isolation from the rest of mankind.

so In all stages of life, there are people who deserve our thanks:

The first people to thank are the my parents; Because of their credit what reaches the sky. Their presence is a reason for survival and their loss is their loss every thing All thanks to them (may God have mercy on them). To everyone who supported me, my sisters, my aunt, my uncle and his family, thank you all

To my friends to whom I testify that they are the best of companions in all matters. Dear Maryam , Farah, Nooralhuda and Nuha Thanks a lot.

To my dear friend who supported me on my study trip, Karim Amroun, thank you.

## ACKNOWLEDGEMENTS

I extend my sincere thanks to those who honored me in supervising the scientific research, which is one of the requirements for obtaining a master's degree in mechanical engineering with supervision Asst.Prof.Dr Ibrahim KOC. I am grateful to them for all the guidance and assistance they provided to me in completing this valuable research.

I also extend my sincere thanks to the head of the Mechanical Engineering Department Asst. Prof. Dr Süleyman BAŞTÜRK for the valuable directions addressed to me.

Also, I extend my sincere thanks to all ALTINBAS University employees, including professors, technicians, and administrators, and to everyone who works at the university for what they provided us with a positive school climate during the two academic years of my presence on the campus. Thank you very much.



## **ABSTRACT**

# **MODIFYING A GENERATOR AND DESIGNING A SOLAR COLLECTOR**

Marwah AL-DAYYENI

M.Sc., Mechanical Engineering, Altınbaş University

Supervisor: Asst. Prof. Ibrahim KOÇ

Date: July 2021

Pages: (75)

This study provides an illustrative description of a method for optimizing a solar collector through a parabolic trough based on the elasticity of the material. And converting the work of a four-stroke electric generator running on gasoline fuel to a two-stroke electricity generator to be run with steam produced from solar collectors. This study aims to obtain electrical energy from clean energy without polluting the environment and at a low cost compared to other sources.

What has been described here is a variation in the reflective surface, which is a small piece of mirror assembled and installed on a metal plate in the form of a cylindrical trough where it is difficult to control the direction of focus of the rays and switch with a plate of flexible polished aluminum, and place the insulators on both ends of the reflective surface to prevent Temperature leakage. For a generator, to be suitable for running on steam, the spark is canceled in the combustion generators and the inlet valve is positioned so that the steam enters directly without effort to open the valve so that the steam maintains its energy. Also, converting the camshaft responsible for opening the exit valve by adding grease (protrusion) against the direction of the first grease to open the valve twice and make the engine two-stroke.

The solar energy collector tested on three days with different weather conditions and it was found that sunny weather is more productive of sunlight, as the combined temperatures reached 143 °C with a steam pressure of 4 bar during a solar complex of an area of 2 m<sup>2</sup> and the efficiency of the solar collector in sunny weather reached 65.98 % compared to the weather. Wet conditions are weak at 85 °C with a pressure of 2.9 bar.

The efficiency of wet weather is 40.36 %. As for the operation of the electric generator, it requires high temperatures from more than one solar collector, so it was operated using a steam generating station to be tested and proven to be effective and capable of using it. Its efficiency reached about 10.6 % and the number of revolutions was 750 rpm. The steam flow rate 30.46 m<sup>3</sup>/h and the engine power reached 1.19 kW. The power output from the engine 774 J. Since the readings obtained from the two devices are good, they can be used to produce electrical energy.

**Keywords:** Solar energy, Steam engine, Electricity generation.



# TABLE OF CONTENTS

	<u>Pages</u>
<b>ABSTRACT.....</b>	<b>vii</b>
<b>LIST OF TABLES.....</b>	<b>xvii</b>
<b>LIST OF FIGURES.....</b>	<b>xiii</b>
<b>LIST OF ABBREVIATIONS.....</b>	<b>xv</b>
<b>LIST OF SYMBOLS.....</b>	<b>xvi</b>
<b>1. INTRODUCTION.....</b>	<b>1</b>
1.1 PROBLEM STATEMENT.....	2
1.2 THESIS CONTRIBUTIONS.....	3
<b>2. LITERATURE REVIEW.....</b>	<b>4</b>
2.1 THE STAGES OF DEVELOPMENT OF SOLAR COLLECTORS.....	4
2.2 OTHER CURRENT COLLECTORS.....	5
2.3 SOLAR COLLECTOR MODEL CHARACTERISTICS.....	7
2.4 BASIC THEORY AND TERMINOLOGY.....	8
2.5 PARABOLIC-TROUGH COLLECTORS.....	8
2.5.1 Reflective Surface.....	10
2.5.2 Material for Absorber Pipe Foundation.....	11
2.5.3 Pipe System.....	11
2.6 ADVANTAGES OF PARABOLA COMPLEXES.....	13
2.7 DISADVANTAGES OF SOLAR ENERGY.....	13
2.8 MECHANICAL ENERGY SOURCES.....	14
2.9 STEAM ENGINES.....	15
2.9.1 Advantages of Steam Engines.....	16
2.9.2 Mechanism of Steam Engine.....	17
2.9.3 Field of Application of Small Steam Engines.....	17

2.10 CONVERTING A FOUR-STROKE ENGINE TO A TWO-STROKE ENGINE.....	18
2.11 USING A STEAM ENGINE WITH RENEWABLE ENERGY.....	20
2.12 ENGINE DRIVE BY STEAM BY USING PARABOLIC TROUGH.....	20
2.13 LITERATURE SURVEY.....	21
<b>3. METHODOLOGIES.....</b>	<b>25</b>
3.1 REQUIREMENT.....	25
3.1.1 The Requirements for Improving Solar Collector.....	25
3.1.2 Steam Composition.....	26
3.1.3 The Converting a Home Electric Generator.....	27
3.2 BUILDING A SOLAR ENERGY COLLECTOR.....	28
3.2.1 Support Stand.....	28
3.2.2 Supporting Frame.....	29
3.2.3 Radiation Absorber Tube.....	30
3.2.4 Parabolic Trough.....	31
3.2.5 The Final Form of the Solar Collector.....	32
3.2.6 Solar Collector Efficiency.....	32
3.2.7 Steam Flow Inside the Tubes.....	33
3.3 ELECTRICAL GENERATOR.....	34
3.3.1 Design of Steam Engine .....	35
3.3.2 Engine Characteristics after Modification.....	37
3.3.3 Calculations and characteristics of modified engine.....	37
3.3.3.1 Volumetric flow rate.....	37
3.3.3.2 Mass flow rate.....	38
3.3.3.3 Work.....	38
3.3.3.4 Engine revolutions.....	38
3.3.3.5 Efficiency of engine.....	39

3.3.4 Design of Camshaft.....	40
3.4 FINAL FROM OF THE EQUIPMENT.....	42
<b>4. RESULTS AND DISCUSSION.....</b>	<b>43</b>
4.1 CALCULATIONS.....	43
4.2 WATER TEMPERATURE IN THE ABSORPTION TUBE.....	43
4.2.1 Data for the first day.....	43
4.2.2 Data for the second day.....	46
4.2.3 Data for the third day.....	48
4.3 COMPARING THE SOLAR COLLECTOR TO ANOTHER COLLECTOR.....	51
4.4 DISCUSS THE CALCULATION OF SOLAR COLLECTOR EFFICIENCY.....	52
4.5 COMPARISON OF A MODIFIED STEAM ENGINE TO AN ORIGINAL ONE.....	53
4.6 RESULTS AND DISCUSSION OF THE MODIFIED ENGINE.....	54
4.7 SOLAR COLLECTOR TEMPERATURE RESULTS.....	55
4.8 THE FINANCIAL COST AND FUTURE OUTLOOK.....	56
<b>5. CONCLUSIONS AND RECOMMENDATIONS.....</b>	<b>57</b>
5.1 CONCLUSIONS.....	57
5.2 RECOMMENDATIONS FOR FUTURE WORK.....	58
<b>REFERENCES.....</b>	<b>59</b>
<b>APPENDIX A.....</b>	<b>62</b>

## LIST OF TABLES

	<u>Pages</u>
Table 3.1: Sizes used in building support stand .....	28
Table 3.2: Specifications of support frame.....	29
Table 3.3: Specifications of absorber tube.....	30
Table 3.4: Parabolic trough sizes.....	31
Table 3.5: The characteristics of TIGER-TG3700E generator.....	34
Table 3.6: Gasoline and steam engine specifications.....	39
Table 4.1: Specifications of the first day.....	44
Table 4.2: Water test results in dry weather.....	44
Table 4.3: Specifications of the second day.....	46
Table 4.4: Water test results in wet weather.....	47
Table 4.5: Specifications of the third day.....	49
Table 4.6: Sunny weather test results.....	49
Table 4.7: Results of solar collector efficiency and net useful heat gained values.....	52
Table 4.8: The differences between modified engine and another engine.....	54
Table 4.9: Efficiency values of the modified engine.....	55

## LIST OF FIGURES

	<u>Pages</u>
Figure 2.1: An LS-2 type collector module is shown installed on the platform.....	5
Figure 2.2: Front (left) and rear (right) views of LS-3 collector.....	6
Figure 2.3: Rear view of SENERTROUGH collector.....	6
Figure 2.4: Front (left) and rear (right) views of Euro Trough collector.....	7
Figure 2.5: Solar collector assemblies' parabolic trough at a test center for solar testing in Spain.....	9
Figure 2.6: The reflective surface view.....	10
Figure 2.7: Absorbent type stainless steel, a) under the influence of a temperature of 700 °C, b) stainless steel tube view.....	11
Figure 2.8: Examined model of reflectance mirror and tube view.....	12
Figure 2.9: The generator engine view.....	14
Figure 2.10: Steam engine view.....	15
Figure 2.11: The four-stroke engine view.....	18
Figure 2.12: The two-stroke engine view [Fuel-intake position of a two-stroke engine].....	19
Figure 2.13: Water tank, heat absorbing tube, reciprocating steam engine and parabolic trough view.....	21
Figure 3.1: Solar collector with modify generator.....	25
Figure 3.2: Aluminum foil (ATE - 180) view.....	26
Figure 3.3: Wood insulator view.....	26
Figure 3.4: The process of shedding solar rays into the absorber.....	26
Figure 3.5: The electric generator used view.....	27
Figure 3.6: The support stand view.....	29
Figure 3.7: The supporting frame view.....	30
Figure 3.8: The radiation absorber tube view.....	31
Figure 3.9: The parabolic trough view.....	31
Figure 3.10: The solar energy collector view.....	32

Figure 3.11: The TIGER-TG3700E generator view.....	35
Figure 3.12: Schematic view of original (4-stroke) and modified (2-stroke) engines.....	36
Figure 3.13: The modified engine.....	37
Figure 3.14: Electric generator view after modulation.....	40
Figure 3.15: The view of the camshaft on the gasoline engine.....	41
Figure 3.16: The view of the camshaft on the steam engine.....	41
Figure 3.17: The vertical section of camshaft of the gasoline engine.....	42
Figure 3.18: The vertical section of camshaft in steam engine.....	42
Figure 3.19: Final form of the equipment view.....	42
Figure 4.1: Change of water temperature according to time in dry weather conditions.....	45
Figure 4.2: Change of water pressure according to time in dry weather conditions.....	46
Figure 4.3: Change of water temperature according to time in wet weather conditions.....	47
Figure 4.4: Change of water pressure according to time in wet weather conditions.....	48
Figure 4.5: Change of water temperature according to time in sunny weather conditions...	50
Figure 4.6: Change of water pressure according to time in sunny weather conditions.....	50
Figure 4.7: Parabolic solar collector view.....	51
Figure 4.8: Comparing the efficiency of the modified solar collector with the efficiency of its predecessor .....	52
Figure 4.9: Steam engine view.....	53

## LIST OF ABBREVIATIONS

PTCs	:	Parabolic-Trough Collectors
TDC	:	Top Dead Center
BDC	:	Bottom Dead Center
CSP	:	Concentrating Solar Power
DC	:	Direct Current
AC	:	Alternating Current



## LIST OF SYMBOLS

$\eta$	:	Efficiency (%)
$Q_u$	:	Net useful heat (W/m <sup>2</sup> )
$A_C$	:	Collector area (m <sup>2</sup> )
$H$	:	The average solar radiation (W/m <sup>2</sup> hr)
$R$	:	Tilt factor for beam radiation
$m$	:	Mass (kg)
$\rho$	:	Density (kg/m <sup>3</sup> )
$v$	:	Specific volume (m <sup>3</sup> )
$v$	:	Specific heat (kJ/kg K)
$C_p$	:	Heat capacity (J/ kg °C)
$T_{fo}$	:	Fluid outlet temperature (°C)
$T_{fi}$	:	Fluid inlet temperature (°C)
$q$	:	Vapor flow (m <sup>3</sup> /h)
$d$	:	Diameter (mm)
$V_{cy}$	:	The volume of cylinder ( m <sup>3</sup> )
$L$	:	Length of cylinder (mm)
$P$	:	Pressure (bar)
$v_g$	:	Specific volume (m <sup>3</sup> /kg)
$\dot{V}_g$	:	Volumetric flow rate (m <sup>3</sup> /kg)
$N$	:	Number of cycles (RPM)
$W$	:	Work done (W)
$\eta_{carnot}$	:	Carnot efficiency (%)
$\eta_{isent}$	:	The isentropic efficiency (%)

# 1. INTRODUCTION

## 1.1 INTRODUCTION

This study is an illustrated overview of a method based on the material's elasticity for producing a closed parabolic trough solar energy collector package. What is defined here is a manual method for producing high-efficiency solar collectors at very low costs. The most advanced and lowest cost solar thermal technology available today has proved to be parabolic trough technology. As a result, most of the commercial solar thermal power plant construction projects are based on this type of collector; many parabolic trough power plants are expected to be installed in the USA, Spain, North Africa, the Middle East, etc. Any of these plants consists of a solar field, a steam engine, a loop of electricity, and a back-up battery fired by fossil fuel. More future parabolic trough plants are anticipated to have thermal storage systems. [1]

In many applications, solar power can be utilized to provide all or half of their electricity needs. The most popular applications where solar irradiation can be used are space heating and domestic hot water processing at low-temperature levels. Solar cooling, desalination, and industrial process heat are applications that can utilize solar energy at medium temperature temperatures, primarily with highly efficient collectors such as parabolic trough collectors. Concentrated solar power plants are applications that are attracting more worldwide popularity at high-temperature levels. Also, processes such as hydrogen manufacturing and methanol-reforming use solar irradiation for exceptionally high-temperature amounts of up to 1000 °C. Also, solar collectors can be used to support gas turbines reach elevated temperature ranges, minimize system running costs and deliver cleaner energy. The majority of medium and high temperature applications use parabolic trough collectors to provide the necessary heat. [2]

At its source, the Sun, where its radiance is around 63 MW/m<sup>2</sup>, solar radiation is a high-temperature, high-energy source. However, on the Earth's atmosphere, Sun-Earth geometry significantly limits the flow of solar energy down to about 1 kW/m<sup>2</sup>. Nevertheless, this limitation can be resolved by using concentrated solar systems that convert solar energy into another source of energy under high solar flux (usually thermal). In the spotlight of solar thermal focusing devices, solar radiation is converted into thermal energy. These devices are categorized as either point-focus concentrators (central receiver systems and parabolic dishes) or line-focus concentrators (parabolic-trough collectors (PTCs) and linear Fresnel collectors) by their focus geometry. On the collector axis, PTCs concentrate direct solar radiation on a focal line. This focal line is equipped with a receiver tube with a fluid flowing inside that collects concentrated solar energy from the tube walls and increases its enthalpy. To ensure that the solar beam falls parallel to its axis, the collector is fitted with one-axis solar monitoring. Only direct solar radiation, called beam radiation or direct normal irradiance, may be used by PTCs, i.e. the proportion of solar radiation that is not deviated by clouds, fumes, or dust in the atmosphere and which as a parallel beam enters the Earth's surface [3].

Any solar thermal energy collector's operation can be defined as an energy balance between the collector's absorbed solar energy and the collector's removed or lost thermal energy. If no alternative method for extracting thermal energy is given, the heat loss of the collector receiver must be equal to the solar energy absorbed. Until the convective and radiation heat loss from the receiver equals the absorbed solar energy, the temperature of the receiver increases. The temperature at which this happens is called the temperature of the stagnation of the collector. Active heat removal must be used to monitor the temperature of the collector at a point cooler than the stagnation temperature. This heat is then made available for use in a solar power plant. The rate at which heat is actively extracted from the collector determines the operating temperature of the collector. The amount of heat lost from the receiver must be kept low for the removal of a significant fraction of the absorbed solar energy as usable heat [4].

The dominance of internal combustion engines has been challenged by fuel prices and tighter emissions standards. Hence the idea of using solar collectors and the high temperatures obtained from these collectors to produce electrical energy at lower costs and less harmful to the environment. As the main idea here is to modify a four-cycle household fuel-powered electric generator and turn it into a two-cycle steam-powered electric motor that is obtained from solar collectors in order to take into account the cost needed to produce electrical energy from internal combustion engines and also to reduce the damage generated by them [5].

## **1.1 PROBLEMS STATEMENT**

Problems can be encountered in the following stages of the process of generating electrical energy from parabolic solar collectors

- i. Designing a solar collector and improving its working conditions and reducing losses in the accumulated temperatures.
- ii. Converting a gasoline four-stroke internal combustion engine to a two-stroke external combustion steam engine.
- iii. Producing electrical energy from the collected sunlight to reduce the toxic emissions associated with the combustion process.

## 1.2 THESIS CONTRIBUTIONS

Several contributions are provided in this study that has have not been presented and clarified in the current literature such as:

- i. Explaining how to design a parabolic solar collector.
- ii. Optimizing the solar collector to achieve greater reflection of the sun and reducing heat losses.
- iii. Modifying the camshaft of a four-stroke engine to two-stroke engine's one.
- iv. Study of converting a small four-stroke fuel generator into a two-stroke steam generator by changing the principle of operation of the combustion chamber.
- v. The ability to use clean energy to generate electricity at the lowest costs.

## 2. LITERATURE REVIEW

### 2.1 THE STAGES OF DEVELOPMENT OF SOLAR COLLECTORS

The first solar collector was 3.25 m<sup>2</sup> and was powered by a 373 W pump that produced steam inside the solar collector (today it is called direct steam generation or DSG). Seven more systems were developed after that, this time with air as the working fluid. Ericsson has built a large "solar engine" on display at the New York Exposition that consists of a 3.35 × 4.88 m pool collector that concentrates solar energy into Boiler tube is 15.88 cm long. Sticks supported the capacitor, which was attached to the edges of the sink by parabolic curved iron ribs. These sticks have mirror panels made of smooth window glass with a silver bottom. This device is purely manual in its monitoring of the sun. During summer testing, the average engine speed was 120 rpm, and the absolute piston operating pressure was 0.24 MPa. For security reasons, Ericsson refused to reveal his technical knowledge of the boilers, died before a commercial version of the Sun Engine was built, and his plan was never realized.

Several years later, American inventor Frank Schumann developed and tested a number of solar engines. Frank Schumann used deconcentrating, low-concentration solar collectors (absorbers with flat reflector wings). In Tacon, Pennsylvania (USA), some of them were used for pumping irrigation water. Schumann designed and built a huge irrigation pumping station. Schumann then teamed up with Charles Vernon Boys, an English expert who advised major revisions to the set's design. To adjust the focal axis of the parabolic trough complex, they used glass-covered boiler tubes. The absorber receives 0.1 MPa saturated steam directly from the solar collectors. From north to south, each of the five rows of a similar pool complex is 62.17 m long and 4.1 m high, with a total pool size of 1250 m<sup>2</sup> and a total floor surface of 4,047 m<sup>2</sup>. Suction tubes with a diameter of 8.9 cm and a concentration of 4.6 have a maximum efficiency of 40.7 %. [3]

## 2.2 OTHER CURRENT COLLECTORS

Other power generation solutions based on the Euro Trough concept have recently appeared. The basic idea is to retain some engineering parameters while optimizing benefits and reducing costs through the use of readily available components. This philosophy is shared by the following collectors:

The US Company Solargenix Energy collaborated with the Department of Energy (DOE) in 2003 to develop solar collectors (SGX1 and SGX2) with the goal of increasing efficiency and reducing costs. The SGX1 complex was generated first, followed by the LS-2 complex, which can be twice as long. As a result, the variables (mirrors and receivers) are identical. The lightweight zone frame construction of the SGX1 collectors is custom made entirely of aluminum for easy storage, transportation and management during production and field installation, as well as being waste resistant. This complex also includes newly designed and later upgraded subsystems such as sun tracking controls, steering towers and command units. Compared with the previous generation sinks, the overall performance is improved by 10% with a 20% reduction in cost. The ability to reduce technical time is one of the most important talents associated with the second generation, the SGX2. The Spanish company Solargenix Energy used SGX2 collectors in 55 % of its products in 2006. Figure 2.1 shows the LS-2 solar collector installed on the platform produced by the American company Solargenix Energy in cooperation with the department of energy (DOE) to build the solar collectors [3].

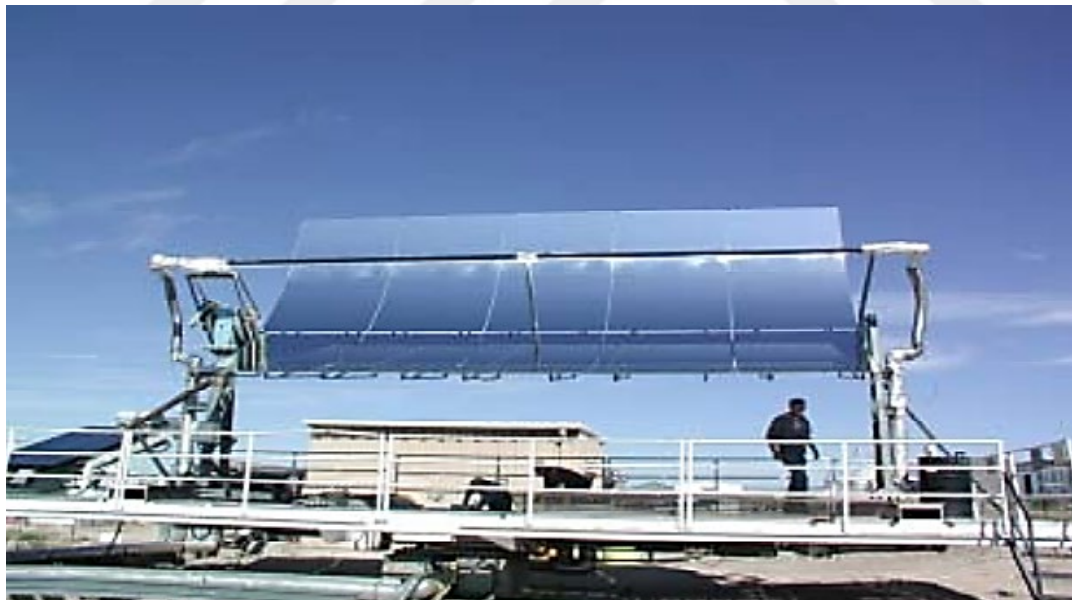


**Figure 2.1:** An LS-2 type collector module is shown installed on the platform [6].

Spanish company SENER is known for its similarly sized SENERTROUGH-I solar collector designs, as are the LS-3. On the other hand, the add-on chassis is designed around the concept of the LS-2 torque tube. When metal is destroyed, the cylindrical tube is made of a very hard material that varies in depth before being struck according to the needs of the concavity setting. Cantilever arms, constructed using sheet metal printing techniques, attach mirrors past the average torque tube, resulting in a 30 percent reduction in manufactured, installed and total charges.

In 2005, two prototypes were tested at plataforma solar de almeri´a (PSA), where a 600-meter full-loop complex was constructed inside the Andasol-1 concentrating solar power plant (Granada, Spain) to ensure it was operational. This complex was selected again in addition to the buried Extresol-1 concentrating solar power (Extremadura, Spain). In partnership with problem-solving vendors, the latest generation of SENETROUGH2 (Flabeg Solar International or SCHOTT) has been created. Figure 2.2 depicts the LS-3 solar collector installed on the platform, while Figure 2.3 depicts the SENERTROUGH-I solar collector manufactured by SENER in Spain.

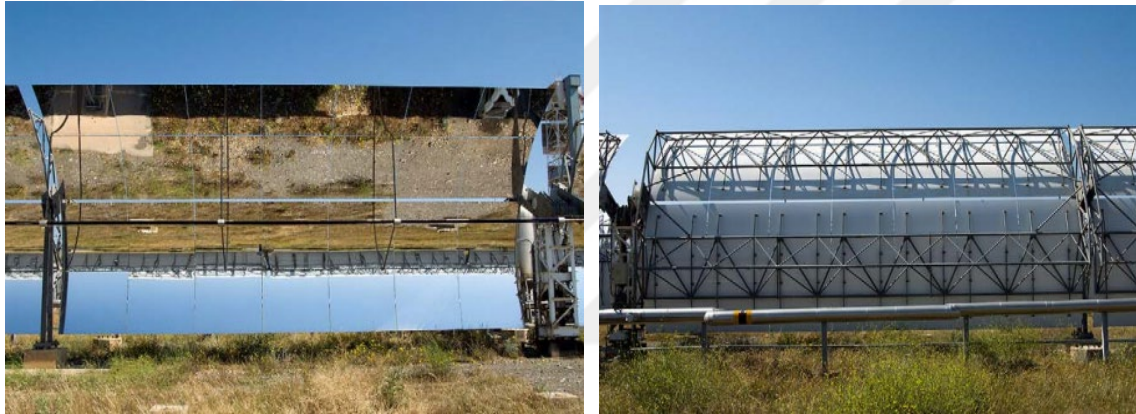


**Figure 2.2:** Front (left) and rear (right) views of LS-3 collector.



**Figure 2.3:** Rear view of SENERTROUGH collector.

Albea Solar (Spain) has thrived in the construction and design of several solar collectors, but it has experienced a current collector known as the El Paisa Basin. Again, the shape is identical to the LS-3 complexes, but the graph concept is similar to LS-2. The main difference beside the Sener diagram is the torque tube of the solar collector. In this case, the cylindrical rod is taken with respect to the IV 908 arc parts (made of cold-rolled galvanized metal profiles) along the half-assembled plates with screws. The tool is hot galvanized steel. This unique torque barrel idea provides a highly boxed part with extended torsion and bending difficulty but cuts manufacturing time yet cuts costs.

The Italian National Center for Environmental and Renewable Research (ENEA) is upgrading a modern parabolic trough collector equal to the bulk of the LS-3 complex. The condenser is a parabola with larger sides than the conventional ones (half a parabola) and is meant to have a maximum accumulated heat of 550 °C [3].

### 2.3 SOLAR COLLECTOR MODEL CHARACTERISTICS

In that study, work was done on a Euro Trough ET-150 solar collector, which is a widely known commercial parabolic collector. This solar collector has been used in many studies and applications and that is why parabolic trough collector was chosen. The concentration of this collector was about 26.37, which is a typical value among commercial parabolic trough collectors. As for the main parts of this collector is the base, reflector and evacuated tube. The reflective surface can also be made by bending a polished and smooth reflective material into a parabola. The evacuated tube consists of a cover glass and a selective absorbent. Between the absorber and the cap, there is a very low pressure of some millibars in order to eliminate the heat load loss of the absorber, and this is a fact that increases the thermal efficiency of the solar collector. Moreover, there are other important characteristics of the solar collector, such as emissions, ambient conditions, optical efficiency and intensity of solar radiation among others. Figure 2.4 shows the Euro Trough ET-150 solar collector installed on the platform [2].



**Figure 2.4:** Front (left) and rear (right) views of EuroTrough collector [2].

## 2.4 BASIC THEORY AND TERMINOLOGY

One of the most important types of photovoltaic solar collectors is the parabolic trough. This is designed from a long parabolic mirror (usually covered with brushed aluminum) along with an absorbent tube running at the center point along the collector. Where sunlight is reflected through the reflector, which directs the solar rays towards the absorbent tube. Usually, a tracker that tracks the sun's rays north-south or circular according to the solar tracker is added every day. Alternatively, with respect to the east-west axis, the basin may remain additionally aligned; this lowers the throughput of the appropriate volumes of the collector according to the failure of the cosine, but only agrees the trough after recumbency aligned with the seasonal shift [7].

In general, constant parabolic troughs are generated at low ratios on the concentration of photovoltaic. To absorb bright sunlight, alternate warmth by thinning flows through the absorbent. In the engine, the heat transfer becomes to heat the steam. This method is sparing and the extreme effectiveness varies beyond 60-80 percent of tube heating. The standard efficiency, i.e. (electrical output power) / (total solar power), collector side after grid is about 15 percent. Hybrids are highly developed commercial plants, so they work on parabolic troughs; the use of fossil fuels returns all night long, yet the aggregation around ancient fossil fuels is limited by a cap of 27 percent of the electricity supply, which helps thinking about renewable energy. On the grounds that those hybrid plants are expected to build cooling plants, or condensers, or accumulators, or other things, the sophisticated control of the square meter of the house varies surprisingly with stiffness. [4].

## 2.5 PARABOLIC-TROUGH COLLECTORS

For years, the focus on improving solar energy has been limited by a mix of operational challenges, assembly costs, and obnoxious fat prices. The focus of the solar base has emerged as a larger potential option due to large-scale electricity generation coupled with modern features among technologies, optics, systems and controls, along with a renewed understanding of the cost on renewables. Parabolic photovoltaic technology, as well as large-scale concentrating solar power control technology and possible baseline cost, have stabilized the science [6].

It has demonstrated recently accessible semi-advanced or fundamentally valuable photovoltaic energy according to residual parabola basin technology. As a result, most of the indoor construction tasks of industrial PV heat reduction are mainly based on this type of collector; it is expected that bushy equivalent plants installed to control conditions in USA, Spain, North Africa, Middle East, etc. Rocket fuel battery [1]. Solar electricity may cover a large area of electricity requirements, especially domestic hot water generation, home heating, and the demand for manufactured heat, then generated by electricity in solar power plants [8].

The design of PV heat collectors is a multivariate optimization process due to the fact that many planning parameters have to be different and optimized with respect to a project-specific foundation, especially the area over the collectors and storage volume. The cost related to the facilities of solar energy structures in the township heating networks has been mentioned for a long time. Fixed Price Energy (LCOE) is becoming the common or near-common criterion for selecting technologies close to proprietary means to manufacture energy on an ongoing basis. The LCOE now focuses not only on the cost related to electric power generation structures, but also on energy production from the regulations that were simultaneously examined. Planar virtue of warmth (LCOH), which is derived from LCOE, is obsolete as its use increases consistent with the photovoltaic warmth of city solar heating collectors. The concept of LCOH remains old as a tool to help accomplish determinations on systems layout, but the schematic diagram is entirely dependent on improvement endeavors and concentrated solar power development. Figure 2.5 concentrating solar power shows a parabolic trough at the solar test center in Spain [9].

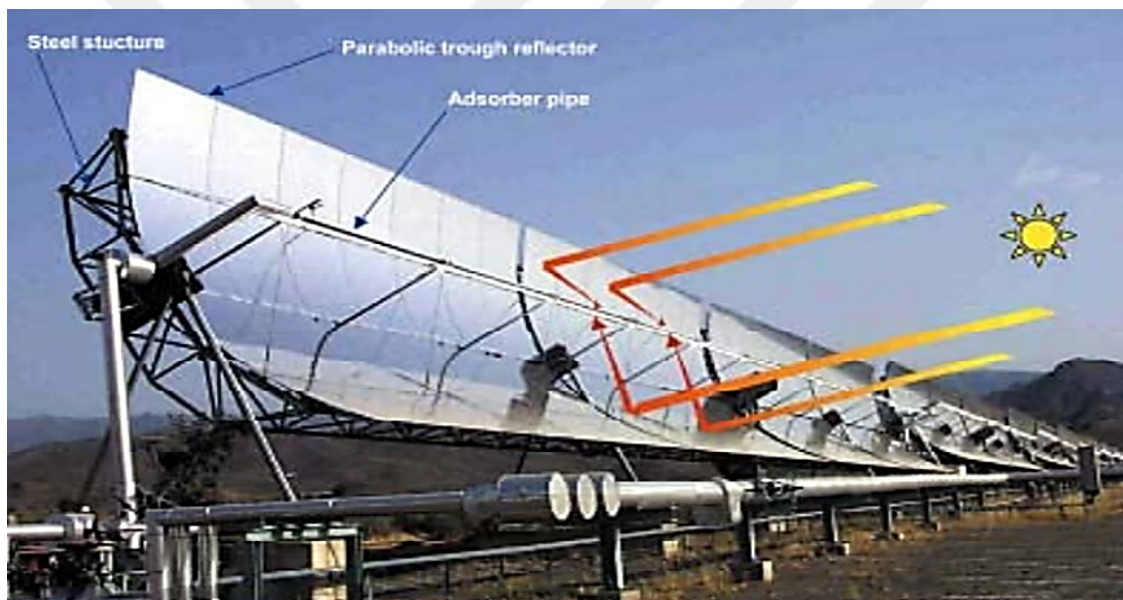


**Figure 2.5:** Solar collector assemblies parabolic trough at a test center for solar testing in Spain [6].

The reflecting mirror of the sun's heat, the absorption tube and the foundation are also one of the most critical aspects of the solar collector.

### 2.5.1 Reflective Surface

The reflection of the mirror has a great and severe effect on the performance of the solar collector. For example, a limit of about 0.15 between reflections at molten heat by heat transfer up to 400 °C reduces the efficiency of a solar collector by about 24.5 %. This indicates that differences in models' predictions of sunlight can be explained simply by using half-errors between repeated reflections. Neglecting 5 % of the reflection, for example, might provide an explanation for the 7 % performance curvature. This research is also in line with the increased value of keeping mirrors on the sinks, but the glass envelopes around the heat-collecting element are clear. Reflection is so convenient with the reflector instrument that each study measures exactly a small factor with respect to the mirror; accordingly, the readings are based on the technical body of a half-sample simulation, which is a very large sample to mimic the actual collected reflective display of a sun collector. Figure 2.6 shows the reflective surface of a parabolic trough solar collector and it made from mirror.

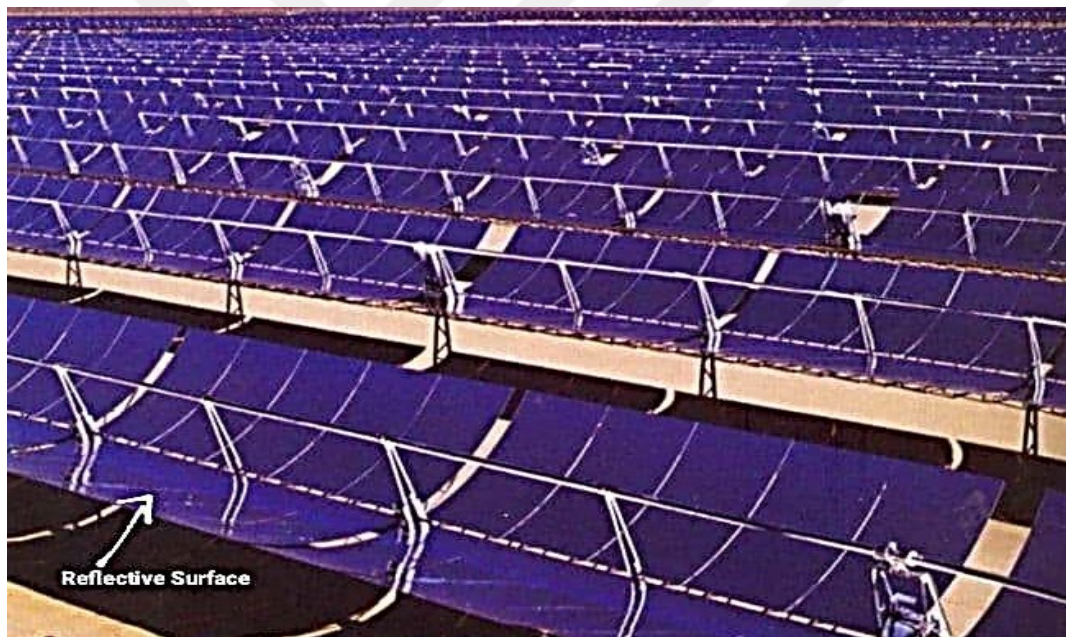


**Figure 2.6:** The reflective surface view [10].

### 2.5.2 Material for Absorber Pipe Foundation

There are 4 materials that can be used to make straw, which are triple non-deformed steel sheets: 321H, 316L, and 304L; with a little copper: B42, shown in the figures below. The materials were selected according to the results on the lowest cost and acceptable efficiency in the production of tube solar collectors. Heat resistance, hardness and ease of heat transfer are among the characteristics of straw materials. However, consistent with the determination of the absorbent rod bottom material, some defects lie in the nature of the material such as weaving strength, loss characteristics, installation amenities, cover application, and charges. Leading to weak and weak adsorption, the heat collector element model uses an ideal solid 321H in the composition of the absorbent part. It was chosen due to the fact that the problem of bending is completely excessive and deceptive, and due to the fact that this slows down the dose related to the durability of the hydrogen contained within. There are other assemblies that use stainless steel as in the manufacture of the absorbent tube used in this study. Figures 2.7 show the materials that can be used to make the absorbent tubes used in solar collectors, which is stainless steel [6].

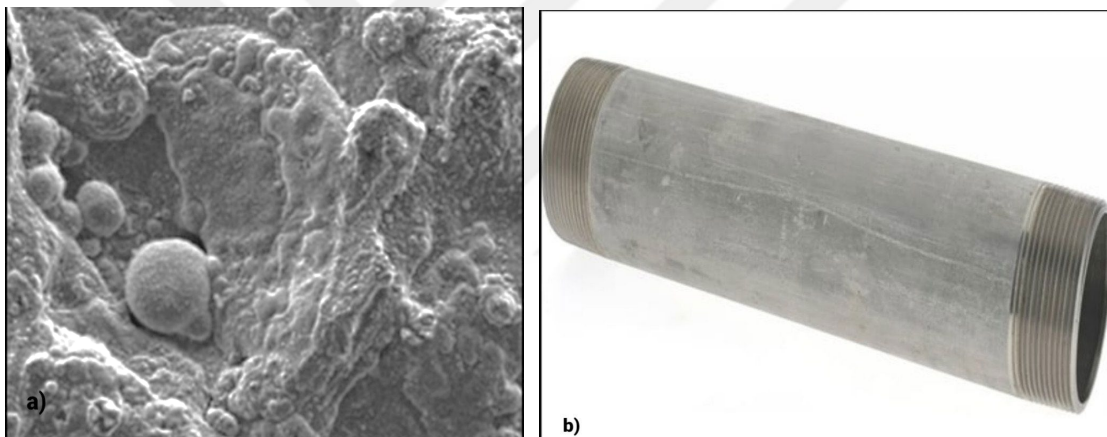


**Figure 2.7:** Absorbent type stainless steel, a) under the influence of a temperature of 700 °C, b) stainless steel tube view [11].

### 2.5.3 Pipe System

The heat exchange fluid flows through the supply tubes with the help of the possibility of connecting pumps, to each section of the header tubes, keeping the fluid pressure above 14 bar in all tubes, to avoid sudden thin evaporation or weak steam generated inside the tubes. (Therminol vapor stress at 400°C is about 12 bar.) This pumping force has a high potential to be controlled by feed water, condensing and cooling pumps, in such a large reach that all this consumption of electrical energy is subtracted from the body through the control block. Head tubes are required depending on the order of heat transfer generated in the solar field. The chosen shape of the piping system depends on maintaining the average velocity along the length of the cylinder. This feature includes a change in the theoretical rod diameter at each epoch in which the floating material

changes. If the material travels with the flow according to equal rings, then the diameter of the barrel head decreases, because the sliding of the shot material follows a pair of rings, which increases the diameter of the head rod. In fact, the diversity with respect to one of the eye diameters is limited to a third or four, depending on the size of the solar field used, and remains consistent with positive complexities. In a step forward, the coordination velocity was set to 2 m/s, in both cold tubes and then hot head tubes. This value was defined as any design value close to optimal. In sections of adjacent loops, a standard T-tube is used, through which the floating part moves in imitation of loops; Sharp opening / contraction inside the tubes, the diameter of the tube changes. In the second step, the exceptional industrial triple diameters were adopted, because both the vertical and the warm tubes, especially at temperatures up to 1000 °C, 1600 °C and 2400 °C, are in a certain way for this quantity at a floating speed within the tubes of less than 2 m/h. This results in a pressure drop and hence heating deprivation resulting from these simulations approximately no more than those outside the theoretical diameters. Therefore, a piping system must be chosen that maintains a high flow velocity inside it and thus maintains the pressure of the generated steam in order to be exploited more widely. Figure 2.8 The following is a schematic model of a parabolic cylindrical solar collector and it shows all the parts with some of the reflecting mirror, absorbent tube, solar radiation and also the base bearing of the collector [1].

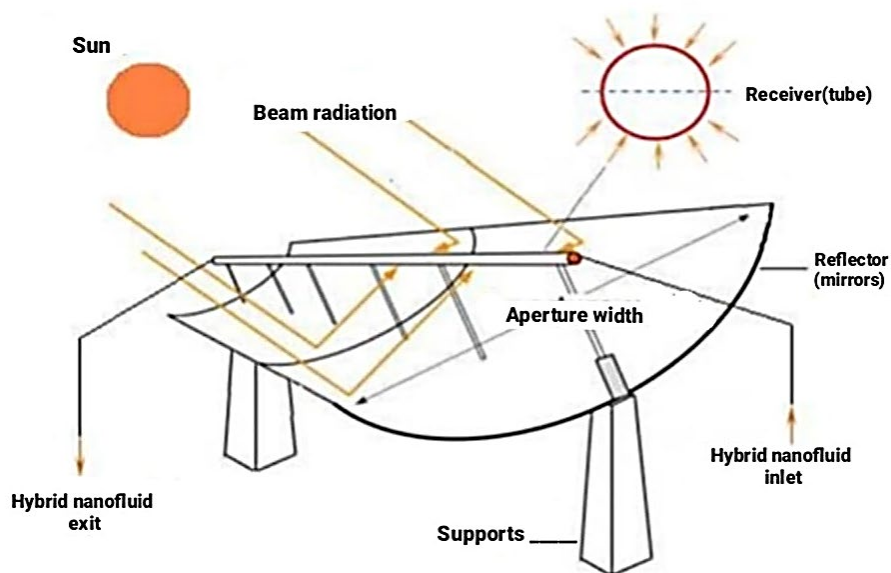


**Figure 2.8:** Examined model of reflectance mirror and tube view. [12]

## **2.6 ADVANTAGES OF PARABOLA COMPLEXES**

Reflective roofs require less material, cost, and are easier to build than flat panel assemblies. It also has several important characteristics, including:

- i. The absorption area of a condenser system is less than that of a flat panel system with the same solar collector system.
- ii. Heat loss in the surrounding area per solar accumulator is less than in a flat panel.
- iii. In the condenser accumulator, the working fluid can exceed high temperatures.

## **2.7 DISADVANTAGES OF SOLAR ENERGY**

- i. Solar electricity systems are very expensive to build if they are built for domestic use, and then there is a great diversity that does not match the uses of solar electricity for non-public or personal things.
- ii. The performance of solar power continues only during the day, so it cannot remain continuous and reliable throughout the night, that is, at sunset, because the sun is the main axis in the production of energy.
- iii. Care must be taken with regularly illuminated photovoltaic panels; however dirt and objects up to expectations hinder reflection beside sunlight and must be removed, so they require constant cleaning.
- iv. Solar panels cannot be placed in confined places and far from sunlight or shadowy places [4].

## **2.8 MECHANICAL ENERGY SOURCES**

Most power generators are powered by oxidizing chemical combustions that emit heat and smoke to produce mechanical energy. These generators are of two types, the first being the internal combustion engines that burn fuel to convert chemical energy into mechanical energy[13]. This type of engine has two types: Engine Spark-ignition, which uses the spark to ignite the gasoline fuel [14], and Engine for compression ignition, which uses pressure heat to start ignition and combustion of fuel and is called diesel engines [15].

The second type is the engine external combustion, in which the combustion takes place outside the engine's cylinder in the presence of air, as in Stirling engines. Mechanical energy [16], and turbine and steam engines, the world has recently turned to external combustion engines to reduce environmental damage and is less expensive [17]. With the increasing use of fossil fuels nowadays, not only on the verge of exhausting the fuel, but also by using it on a large scale, it pollutes the environment which leads to an increase in global warming. There are already millions of cars on the roads, electric motors and other causes of pollution, so it would be irrational to stop the work of these

plants and machines, so it is better to modify the internal combustion engine into an efficient steam engine with minimal cost. The engine used here is the electric generator engine type Tiger TG 3700E, which is shown in the figure 2.9 below. Where it is being developed to facilitate its use with clean energy [18].



**Figure 2.9:** The generator engine view [19].

## 2.9 STEAM ENGINES

The steam engine is used to transform the energy in the steam into the mechanical action used to drive the pump. Steam fills the engine cylinder at high temperatures and pressures, allowing the internal piston to reciprocate, moving the connecting rod back and forth. The connecting rod attaches the crankshaft to the piston at this location. The crankshaft converts its rotational energy to the flywheel, which is a spinning mass, with a large moment of inertia. The flywheel stores energy and provides the angular momentum needed to transition between expansion and compression in the cylinder. The camshaft is a revolving shaft that controls the opening and closure of valves and is operated by a mechanical linkage from the crankshaft. Valve timing is critical for regulating the time of engine revolutions and maintaining proper steam engine operation. A gear coupling and a common joint be used to move the torque from the crankshaft to the drive shaft attached to the water pump; the two shafts be perpendicular to each other [20].

There are a lot of differences in the details although it can be very handy for steam engines but most of them have more components than a similar internal combustion

engine. Figure 2.10 is an illustration showing the mechanism of the piston movement inside the combustion chamber of a steam engine, as when steam enters the pressure, it compresses the piston downward and as a result, a reaction force occurs that pushes the piston back into the piston again [21].

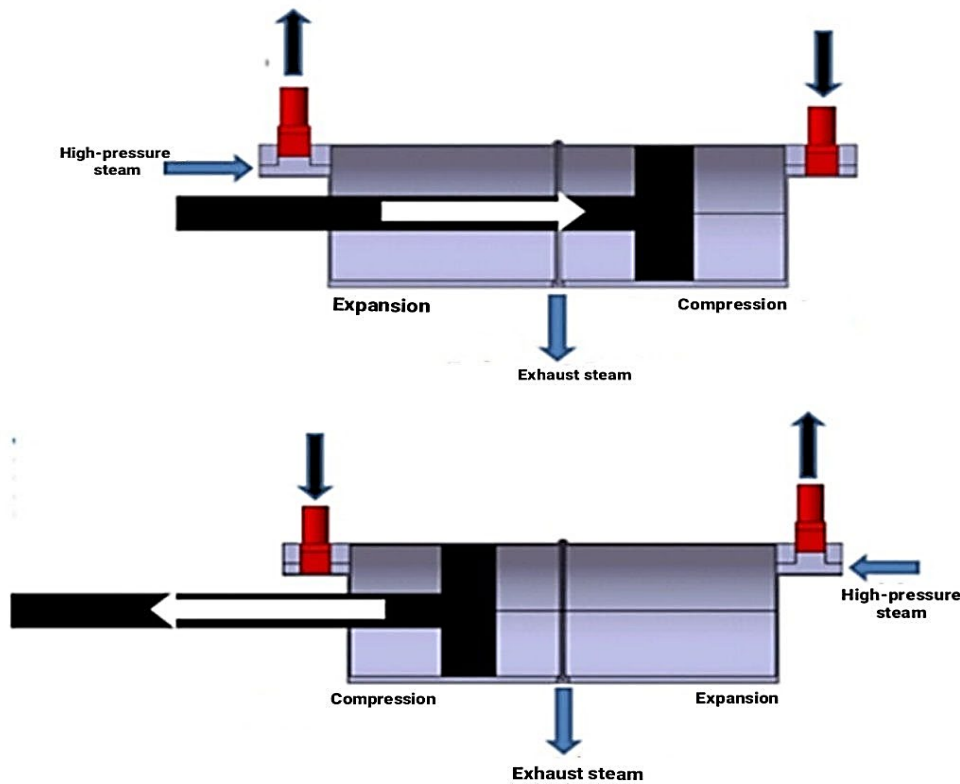


Figure 2.10: Steam engine view [22].

### 2.9.1 Advantages of Steam Engines

The steam engine is similar to the work of combustion engines in many ways, but it has several advantages that make it better than internal combustion engines, the most important of which are:

- i. It has a low cost because it simply does not need fuel, and therefore it does not leave any waste during work and thus is environmentally friendly.
- ii. The temperature generated during the operation process is not very high and therefore it does not need a cooling system
- iii. It is also possible to reduce the properties of the materials used in the construction of its parts and to use materials with low strength and low thermal resistance compared to the materials used in the manufacture of combustion engines, and thus the cost can be reduced as well.
- iv. The used steam can be recycled and used again, and this cannot happen in fuel engines.
- v. Manufacturing and maintenance costs are very low.

- vi. Tanks can be refilled in a very short time compared to the battery that is charged.
- vii. The cost of filling steam-powered vehicles is much cheaper than diesel, gasoline or biofuels [23].

### **2.9.2 Mechanism of Steam Engine**

In a combustion engine, the charge enters the inlet valve during the suction stroke and is compressed by the piston during the compression stroke as the crank rotates. Then, through the spark plug, sparks fly, the gasoline ignites, and the expansion stroke begins, followed by the exhaust stroke, which ejects the combustion product from the engine.

Steam is taken here, compressed and fed into the engine cylinder, where the piston must be at TDC, and the inlet valve and exhaust valve are temporarily closed. When a small rotation of the crank is applied, the compressed steam fills the clearance volume, and the piston begins to slide down as the compressed air expands and pulls the piston down. In one stroke, the piston goes from TDC to BDC. The exhaust valve now opens, and the volume of steam inside the steam-filled cylinder expands and drives the piston from BDC to TDC. In this way, only one two-stroke mechanical kinetic energy production process ends [23].

### **2.9.3 Field of Application of Small Steam Engines**

Off-grid concepts that allow small homes or businesses to be self-sufficient in terms of utilities (electricity, sewage, information flow) that require expensive networks of wires and pipes are gaining in popularity. Small steam engines can be useful in the combined heat and power industry, as well as for distributed power generation in residential settings. In small organic Rankin cycle units, the organic vapor expanders are predominantly of the helical type. These expanders are designed or adapted from the compressors used in refrigeration units, and typically cover a range of 10-25 kW. The goal is to propose building smaller units ranging from 1 kW. For this purpose, it was decided to reconsider the well-proven commutative operator technology. The use of this machine as a steam expander dates back to the 19th century, and design methods and technical solutions developed significantly in the 20th century; however, using advances in materials and motor control systems derived from the IC motor sector, the technology can be revisited. Valve opening and closing can currently be largely controlled by electronic/hydraulic systems; direct current production of electricity in small volumes, which is possible with variable speeds; For large-scale production, it is also possible to consider adapting the existing drive IC or using existing manufacturing lines. [24].

## 2.10 CONVERTING A FOUR-STROKE ENGINE TO A TWO-STROKE ENGINE

To convert a four-stroke engine to a two-stroke engine, one must first understand how a four-stroke internal ignition engine works. A four-stroke engine, as the name implies, has four unique strokes: a suction stroke, a compression stroke, a control stroke, and a smoke stroke. The transmission of a piston between TDC and BDC is referred to as a stir. In addition, the internal combustion engine has two valves to synchronize cranking: an inlet valve and an outlet valve. The inlet valve regulates the flow of the air-fuel mixture into the engine compartment, and the outlet valve regulates the flow of spent gases out of the barrel compartment. When the piston is at TDC, you start the first stroke of an ideal internal combustion engine. The engine inlet valve also begins to open at this point. The piston moves from TDC to BDC during the suction stroke, causing the pressure to drop above the piston head and suction formation. As a result, the air-fuel composition is sucked into the engine compartment when the inlet valve opens during the intake stroke. When the cylinder reaches the BDC, the second stroke begins.

The engine outlet valve is now closed and remain closed until the end of this stroke. The piston advances from BDC to TDC during the stroke. The air-fuel mixture and weight inside the engine compartment increase as the cylinder progresses from BDC to TDC. When the piston returns to TDC, the third stroke begins.

The spark plug located inside the engine compartment causes the air-fuel mixture to ignite at this point. When the air-fuel mixture ignites, the pressure inside the engine compartment rises rapidly. This high-pressure action acts on the piston, pushing it from TDC to BDC. The movement of the piston causes the engine to produce output power, which is why this stroke is called a power stroke. When the piston is at the BDC, the fourth point begins. At this point, the engine outlet valve also begins to open. The piston moves from BDC to TDC during the exhaust stroke, forcing the burning gases out of the engine compartment through the outlet valve hole. For the exhaust stroke, only the outlet valve opens. The lower end of the piston is connected to the crankshaft of an internal combustion engine. The crankshaft rotates 90 degrees per stroke of the piston. Figure 2.11 shows the work of the four strokes in a four-stroke internal combustion engine, which are the fuel ingress, compression, explosion and expansion strokes (exit of combustion products) [25].

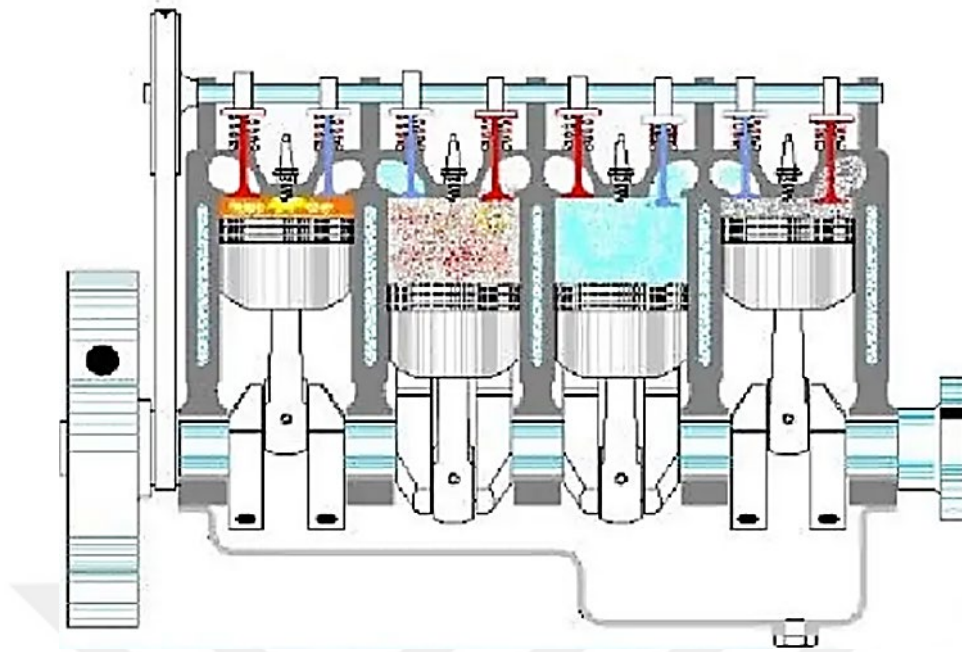


**Figure 2.11:** The four-stroke engine view [26].

During the 4-stroke of the piston, the crank shaft spins for  $720^\circ$  (or two complete rotations). In four-stroke engines, this means that every fourth stroke produces a single power stroke. A power stroke is produced on every second stroke in two-stroke engines. All of these factors were taken into account when converting 4-stroke engines to 2-stroke engines. A 150cc 4-stroke start internal ignition engine was used in this design. To convert this engine to 2-stroke and run it with CAT, the planning gear layout of the cam shaft, bay spout, and valve timing of the engine was changed. Figure 2.12 shows the Fuel-intake position of a two-stroke engine in a two-stroke internal combustion engine, which is the expansion stroke and the compression stroke. Rather than getting a power stroke in elective upheaval, this motor was altered to get a power stroke in each upset of the wrench shaft, and as follows

- i. First and foremost, the cam shaft was changed: originally, the cam shaft was designed to keep a four-stroke engine going by opening and closing an outlet valve at the first and fourth strokes separately. The gulf and outlet valves were closed and opened using this composition .
- ii. Second, the speed ratio of the timing rigging to the wrench shaft equip was changed from 2:1 to 1:1, resulting in an equivalent transformation to the planning gear about the wrench shaft insurgency, resulting in the conversion of a 4-stroke engine to a 2-stroke engine .
- iii. The carburetor of the engine valve is ejected in the third gulf valve change, and a channel spout is added so that the outlet of the compressed air tank can be connected to the Compressed Air Engine .

- iv. Fourth, alter the bay and outlet valve springs: the engine valve carburetor is removed, and a bay spout is added so that the compressed air tank's outlet can be connected to the Compressed Air Engine .
- v. Fifth, the stiffness of the springs used in the valves was eliminated [27].

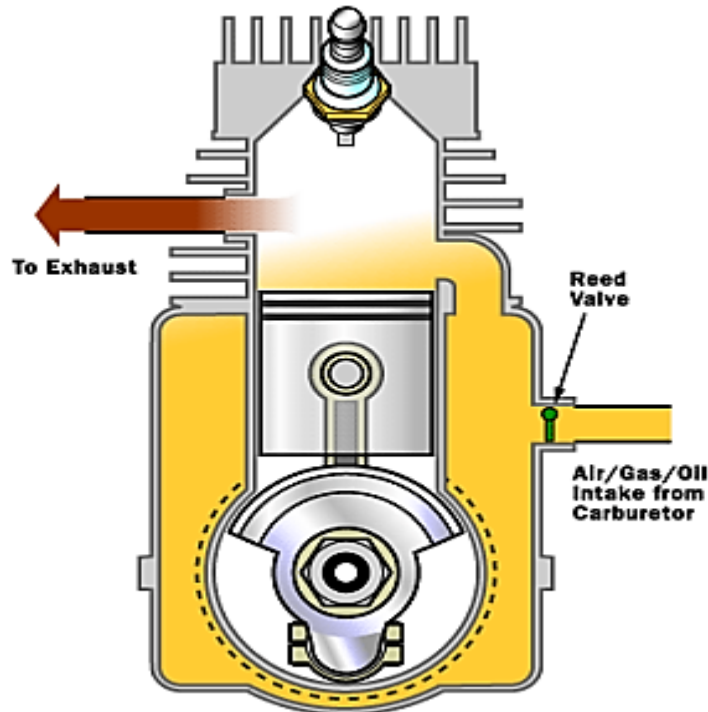


**Figure 2.12:** The two-stroke engine view [Fuel-intake position of a two-stroke engine].

## 2.11 USING A STEAM ENGINE WITH RENEWABLE ENERGY

Solar energy is one of the more appealing renewable energy sources for usage as a heat engine's input energy source. In fact, the reciprocating engine can run on any source of heat energy. The direct conversion of solar energy into mechanical energy minimizes the primary mover's cost and complexity. Because of its basic design and the fact that it is manufactured in the same way as a reciprocating internal combustion engine, the steam engine would benefit from economies of scale and might be created as a low-cost power source for developing countries if mass-produced in huge numbers. The goal is to provide a basic understanding on solar-powered Steam engines as well as a review of available material.

A steam engine is a machine that uses steam as a medium or working fluid to transform the thermal energy of pressured steam into mechanical energy. When water is transformed to steam, it expands 1,600 times its original volume. All steam engines are built on the force generated by the conversion. The basic principle of a steam engine is as follows: A steam engine, like a vehicle engine, includes a piston that moves when

pressure is applied, as well as valves that control the intake and exhaust of the cylinder's contents. Air and fuel are pulled into an internal combustion engine, exploded, and, like a large Rhino in a cannon barrel, strive to escape by pushing on the piston. The inlet valve opens in a steam engine, and steam under pressure pulls on the piston until the exhaust valve is opened to allow it out. While they both feature a piston in a cylinder, valves, and a crankshaft, they are not the same [28].

## 2.12 ENGINE DRIVE BY STEAM BY USING PARABOLIC TROUGH

Water tank, heat absorbing tube, reciprocating steam engine, and parabolic trough make up the system. The water tank is positioned above the absorbing tube's height, and the parabolic trough is positioned so that the sun's concentration is centered on the absorbing tube, producing heat. At high temperatures and pressures, this heat is used to turn water into steam. The reciprocating engine can be started since the pressure is sufficient. Finally, an engine generates mechanical work from sunlight, and it can be used for a variety of tasks such as driving a wheel, producing electricity from a dynamo or generator, running a compressor, and so on. To absorb the focused sunlight, a heat transfer fluid (typically thermal oil) passes through the tube. This raises the fluid's temperature to around 400°C. In a typical turbine generator, the heat transfer fluid is then used to heat steam. The procedure is cost-effective, with a thermal efficiency of 60-80% for heating the pipe [22].

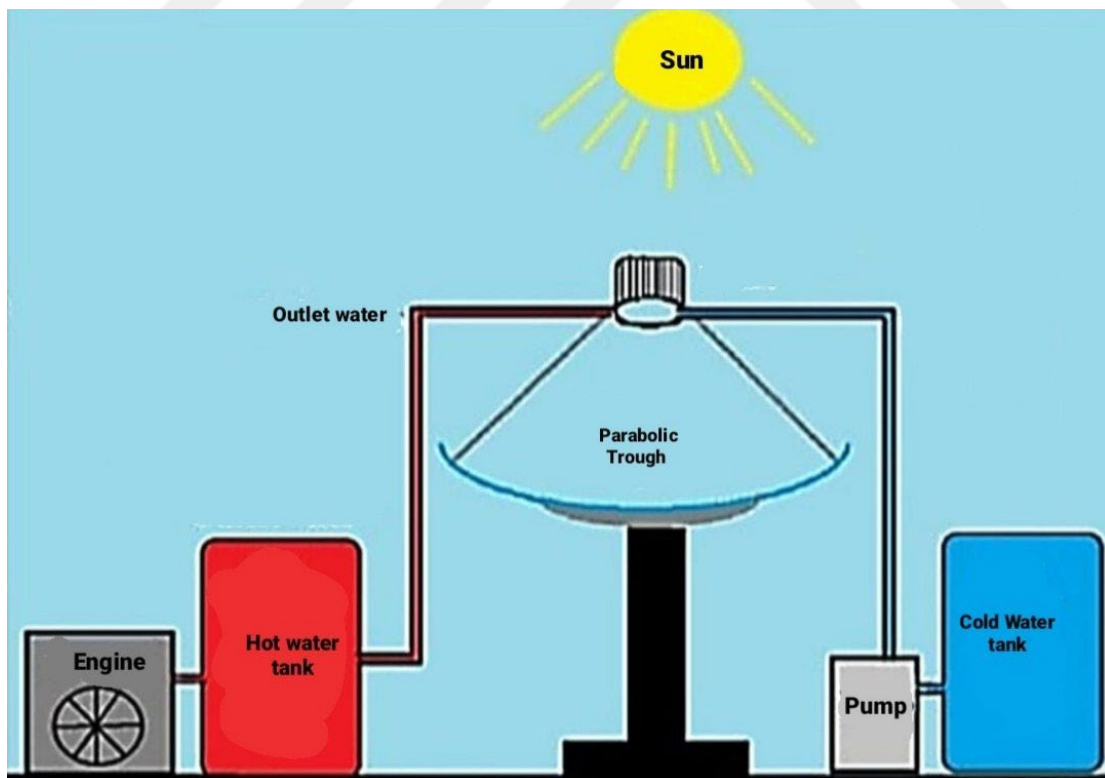


**Figure 2.13:** Water tank, heat absorbing tube, reciprocating steam engine and parabolic trough view [28].

## 2.13 LITERATURE SURVEY

Ferrara G. et al. [24], this paper presents a built-in reciprocating steam extender engine for converting and utilizing low-grade heat resources of many types, such as geothermal energy, solar energy, and waste heat recovery. Non-static pressure and expansion, loss through inlet/discharge valves, and dead vacuum effects are all included in the heat transfer model. The results of this study were compared with the results of the dynamic model, which are based on ideal gas assumptions. The model provides for the calculation and analysis of system performance, as well as its dependence on the main design parameters; it also has a preliminary design with an emphasis on valve sizes. The results show that the proposed technological solution can be implemented and that the performance of the combined heat and power system is comparable to that of other renewable energy technologies. The overall performance of the motor, intended for low-temperature heat sources (solar, geothermal) and small distributed combined heat and power applications (e.g., apartment complexes, possibly in a smart grid arrangement), has demonstrated cycle efficiency of 9 %, and Carnot efficiency (switchable motor). For reflectance) is 17 %. Under nominal conditions, the system achieves an appreciable value of 87 % energy efficiency in terms of the combination of heat and power. The potential for various uses has been demonstrated by sensitivity analysis.

Pradeep Kumar V. R. et al. [4], the overall objective of this study is to look at ways to improve the efficiency of solar energy systems while reducing the cost of electricity or heat produced. The long-term durability and strength of the system was also important to the researcher. Because the basic idea is to maximize the efficiency of the condenser by using powerful, lightweight, and low-cost inverters. In order to increase the performance of the solar concentrator, the researchers considered several geometries and types of inverters in terms of optical and power conversion efficiency. Various types of reflective and absorbent materials were studied in this study to ensure good performance of the focusing system and extended technical life. The optical properties of the reflective surfaces and their degradation were also evaluated. The researchers' interest shifted from evaluating the effectiveness of the concentrated solar collector to examining the optical properties of the reflector and absorbent materials during the research. A finite element model was created for the construction of the solar parabolic trough collector frame and used to verify the structure's ability to absorb torsional and bending forces under dead wind loads. Solar parabolic trough collector and its trace system have been tested in both dry and wet conditions. The obtained experimental results revealed that the characteristic curve of the tested aluminum composite is much lower than that of the mirror collector, where the efficiency of the mirror collector is about 8 % higher than that of aluminum in dry weather conditions.

Bhattacharya S. et.al [29]. In this study a pressure difference as well as a specific temperature distribution across the entire piston is created due to the fundamental nature of combustion in the cylinder of a conventional internal combustion engine. The researcher created and analyzed a piston for a two-stroke spark ignition internal combustion engine with a maximum power of 6.5 kW at 5500 rpm. Here the researcher

used well-established methods to develop the piston, which was built from 4032 aluminum alloy, and then performed a transient thermal and structural analysis. Two alternative designs were examined to improve the piston design by creating slots in the piston flange area. This modification increased the thermal performance of the piston, according to the research. The thermal performance of the alternative design with wide openings in the skirt area was the best. The results of the analysis can be further improved by replicating the actual conditions with the engine combustion model.

Bhamwala B. et al. [18], in this paper, the researchers study the possibility of modifying a two-stroke internal combustion engine that runs on fuel into an efficient air engine powered by clean wind energy at the lowest cost. In this paper a two-stroke internal combustion engine is studied. They find that there are two primary concerns that must be addressed for change. The first is to determine the position of the air supply from a place where the maximum work can be extracted. The other is the timing circuit design to accurately determine the air entry point and air supply duration. The results were satisfactory in terms of cost and efficiency.

Mourya A. et al. [23], the researchers focused on the work of the pneumatic actuator in this publication, in which a compressed air engine uses air as fuel to drive pistons and generate mechanical output without harming the environment. Instead of using typical fuels like gasoline or diesel, the engine runs on compressed air. The air inlet of this compressed air engine is vertical from the top of the piston head. They also changed the camshaft design to alter the valve timing. With this engine, a speed of 60 km / h was obtained experimentally, which is faster than previous work on the same topic. It is also effective because there is no pollution as a result. The experiment also revealed that the car was traveling at a good speed of 60 kilometers per hour, and the extra weight of 18.5 kilograms had little effect on the engine's performance. It also does not pollute the environment. As a result, it is more effective, long-lasting and environmentally friendly.

Reitz R. D. et al. [14], in this article, the researcher explains the value of an Internal Combustion engine, very briefly. Efficiency reduction studies and methods to reduce dependence on fossil fuels are found to be promising avenues for future research into Internal Combustion engine drives. The researcher emphasized that the sources of electricity supply are not fully sustainable and that transportation is not fully electric for many decades. As a result, the researcher emphasized the importance of developing rather than replacing internal combustion engine drives, at least for the time being. Fossil-fueled internal combustion fuel oil internal combustion engines provide around 25% of the world's energy (about 3,000 out of 13,000 million tons of oil equivalents per year) and contribute around 10 % of global warming greenhouse gas emissions. For years, engine researchers and producers have aimed to minimize fuel consumption and emissions. In fact, great progress has been made, making today's Internal Combustion engine drive a technical marvel.

Tian Z. et al. [9], this study presents a general method for optimizing hybrid solar district heating systems based on planar heat cost. The researchers performed the

analyzes on the basis of the isothermal cost of large-scale central solar heating plants. An optimized approach based on Transient systems simulation program – Generic optimization program is introduced. And make multifunctional and functional improvements to the hybrid solar heating plant. The levelized cost of heat for hybrid solar heating plants has also been determined for different scenarios in the near future. The researchers found the net levelized cost of heat for the Taars plant to be 0.42 Danish Krone (DKK)/kWh. The optimized hybrid solar heating plant's net levelized cost of heat is significantly lower than the average heat rate of natural gas boilers (0.57 DKK/kWh). In solar district heating systems, the usage of a parabolic trough collector is cost effective. Solar collectors in district heating networks can reduce the levelized cost of heat system of the Taars plant by roughly 5-9 percent in this study. The findings also suggest that parabolic trough collectors are cost-effective for use in central heating systems. The findings not only give designers with important ideas, but they also result in the lowest heating costs for home end users.

Cristóvão R. et al. [16], this document gives an overview of existing solar energy technologies that can be used to generate electricity either on their own or in conjunction with the main power grid. The researchers go on to present an alternate Stirling cycle-based technology, including its possible applications and limitations. The Free Piston Stirling Engine is being investigated and examined using a fresh conceived design. A literature review of the levelized cost of heat engine was presented, with a focus on the Stirling engine's operation. The Stirling Engine is an efficient technology for integration into small-scale levelized cost of heat systems, whether they are connected to the grid or operate independently, because it is externally heated. The free piston stirling engine system is a simple power conversion heat engine with low maintenance, minimal noise, and a long life. free piston stirling engine is receiving interest from researchers and some current researchers demonstrate a new FPSE design aimed at achieving reasonable thermal efficiency.

Bellos E. et al. [8], the goal of this research is to increase the convective heat transfer coefficient between the working fluid and the absorbent in order to improve the thermal efficiency of the commercial equivalent complex industrial solar technology-parabolic trough collector. The type of working fluid and the sorption geometry, according to the researcher, are the two key aspects that influence this parameter. As a result, three working fluids, thermal oil, thermal oil containing nanoparticles, and pressured water, are investigated. Furthermore, a dimpled absorber tube with a sinusoidal geometry is investigated because this form enhances the heat transfer surface while also increasing flow turbulence. The final findings revealed that these two ways improve the collector's heat transfer efficiency and thermal efficiency. The use of nanofluids, in particular, boosts the collector's efficiency by 4.25 %, while pressured water boosts it by 6.34 %. However, in the case of water, the requirement for a high pressure level in order to keep it in the liquid phase makes nanofluids a more appealing choice. Engineering optimization boosts productivity by 4.55 percent. This implies that these reinforcements are suited for applications involving high temperatures. In these instances, the main

reason for increased efficiency is a rise in the heat transfer coefficient inside the flow, but other parameters like the specific heat capacity of the liquid have a beneficial effect on the collector's efficiency. Furthermore, it is important to note that using an undulating surface increases accumulator pressure losses, which is a component that must be considered in this design.

Mattarelli E. et al. [21], researchers present in this paper a study of the effect of an integrated combustion system on the efficiency of a new 3-cylinder, opposite-piston two-stroke diesel engine, rated at 270 kW (3200 rpm). Because of the higher air-fuel ratios (+20 percent), soot emissions were minimized at full load in the 2-stroke generator. Thanks to internal engine gas recirculation, a decrease in particular NO<sub>x</sub> emissions has been recorded at medium to high speeds. NO<sub>x</sub> is higher at low speed due to accelerated combustion, although it may be minimized by following a separate injection technique. Nearly one-half of the comparable 4-stroke engines are the gross indicated mean effective pressure values: this is a fundamental benefit for injection calibration, as it allows novel combustion concepts to be applied, requiring more independence from cylinder pressure restrictions.

### 3. METHODOLOGIES

The world today worries about protecting the atmosphere and emission control steps have been taken everywhere. Factories and mechanical engines result in a great deal of air pollution. As a result, developers today concentrate on designing environmentally sustainable vehicles that can minimize engine and other vehicle-induced emissions. The role of an engine operating on water vapor, where the engine operates on steam as fuel to push the piston and create a mechanical output without causing any damage to the atmosphere, maybe a significant milestone in this process .

Work was done to create a solar collector in this segment and transform a four-stroke petrol-electric motor into a two-stroke steam engine. This engine is powered entirely by solar thermal power and water, so it is cheap and environmentally sustainable.

#### 3.1 REQUIREMENT

The basic requirements that help in obtaining the electric current from this method are to improve the solar collector with the modified motor, as shown in Figure 3.1 below, the devices used in this study.



Figure 3.1: Solar collector with modify generator.

#### 3.1.1 The Requirements for Improving Solar Collector

To improve and increase the productivity of temperatures and maintain it from dispersion, a flexible metal plate must be used to form aluminum foil (ATE - 180) that is characterized by its resistance to corrosion and high-temperature resistance in addition to a good reflection of sunlight. Figure 3.2, which shows aluminum foil stuck to a metal plate. As for the sides of the solar collector, any insulating surface can be used to

prevent the temperature from leaking outside and to prevent the influence of the wind on the reflective surface, and here a wooden surface with a thickness of 2.5 mm was used for its abundance, as shown in figure 3.3.



Figure 3.2: Aluminum foil (ATE - 180) view.

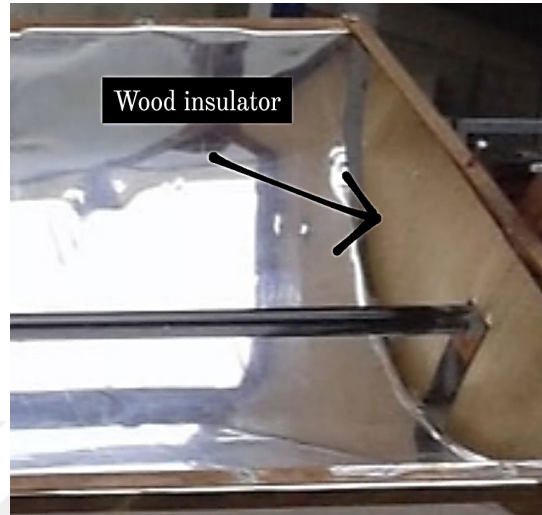


Figure 3.3: Wood insulator view.

### 3.1.2 Steam Composition

The concave reflective surface is used to collect and focus the sun's luminosity and shine it on the receiver located in the center of the focus, which is a metal tube inside which there is an amount of water, which in turn stores temperatures. With the increase in the amount of incident radiation, the temperature of the water increases and the temperature rise until it reaches the boiling point, the water begins to evaporate and transform from its liquid state to the gaseous state, thus forming compressed vapor. Figure 3.4 illustrates the process of shedding solar rays into the absorber.

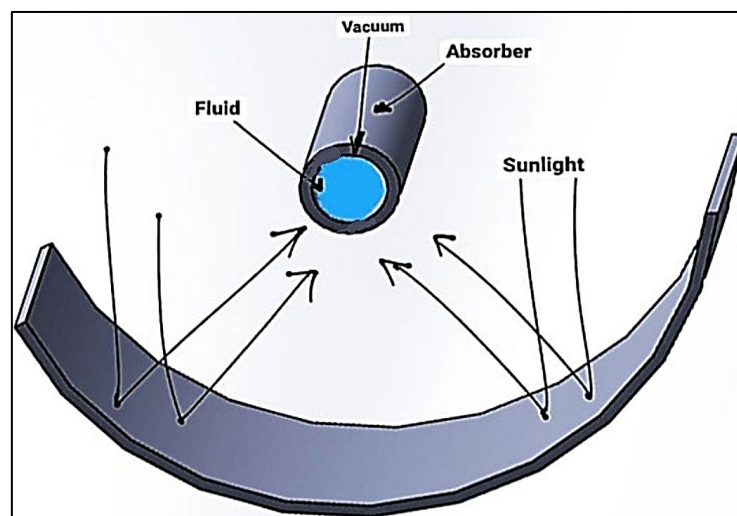


Figure 3.4: The process of shedding solar rays into the absorber.

### 3.1.3 The Converting a Home Electric Generator

The domestic electric generator has been converted to be suitable for working on steam, and this is done by canceling the spark and rotating the camshaft responsible for opening the valves by adding second grease (protrusion) against the direction of the pre-existing protrusion.

This is done by adding a continuous thrust seam welding type welding material, and using an electrode wire in large quantity and in one place on the camshaft at the location corresponding to the previous protrusion location on the camshaft. Then the added part is shaped and made very similar to the pre-existing bump. The process of forming this burr is done using iron filings tools (files), where coarse coils are used to get rid of the hard parts, and when the burr shape is almost reached, the coils are changed with soft files. Soft coils are used more precisely and to make extrusion more smooth in order to facilitate its use and not rub against the internal surfaces of engine parts. Thus the extrusion is formed in a very easy and inexpensive way and this work was carried out in the workshop.

Thus, the valve opens after the camshaft rotates every 180° instead of 360°, so the valves open twice as opposed to their work in the combustion process as they are opened once during the process, Figure 3.5 is the generator used in this study.



**Figure 3.5:** The electric generator used view.

It should be noted here that the method of supplying the solar collector with water is done manually, that is, by opening the suction tube valve from the right side and passing the water inside the tube and then closing the valve. This is a temporary method that was used in this study.

After the steam is formed inside the absorbent tube in the solar collector, it is transferred to the engine cylinder through a heat hose made of rubber with silicon fibers. These hoses are characterized by their extreme resistance to high temperatures and resistance to high pressure.

## 3.2 BUILDING A SOLAR ENERGY COLLECTOR

An illustrative explanation of a method for generating a solar collector through a parabolic trough is given in this part. What be mentioned here is a manual technique for making highly effective solar collectors at a very low price. Which is especially relevant for teaching, researching, or addressing purposes, a solar collector parabolic trough uses a mirror in the form of a parabolic cylinder to reflect and focus light radiation into a receiver tube situated at the parabolic cylinder's focal line. The receiver receives and converts the incoming radiation into thermal energy, transporting and collecting the latter through a fluid medium flowing inside the receiver channel. This concentrated solar collection system has the advantage of high performance and low cost and can be used either for the collection of thermal energy, for the production of electricity, or both, making it an effective way to directly harness solar energy. Technique utilizes a planar plate's inherent elastic deformation to form a curved surface similar to a parabolic cube; the approximation error of this surface is then redressed. The main parts of the solar collector are:

### 3.2.1 Support Stand

The support stand is constructed of steel and consists of rectangular cut belts welded together. Where the stand consists of a right-side holder and a left-hand holder, and they are equal in length, width and thickness. Each of them is installed on a rectangular base after that the support is placed in the middle of the two holders and its dimensions are 2100 mm length, 45 mm width and 30 mm thickness. The following table 3.1 shows the measurements that were adopted in the construction of the support stand.

**Table 3.1:** Sizes used in building support stand.

Dimension	Value (mm)
Height of the support stand (L)	1000
Distance between the two stands (W)	2100
The base length of the support stand (l)	400
Width of the metal used (b)	30
Thickness of the metal used (t)	45

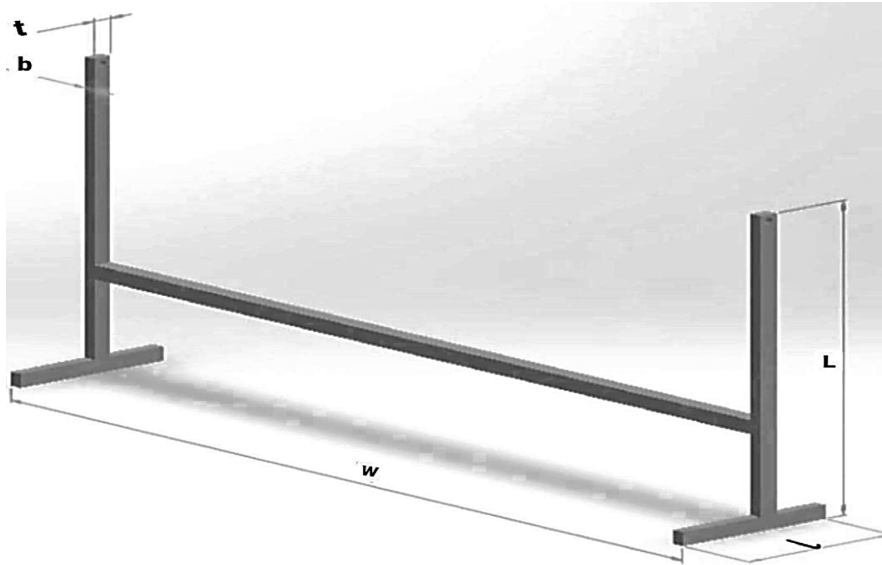


**Figure 3.6:** The support stand view.

### 3.2.2 Supporting Frame

It is the part to which the reflective surface is attached and is fixed at the end of the support stand, and it is constructed of steel and it is a rectangular frame 2000 mm long, 700 mm wide and 30 mm thick. Table 3.2 shows the dimensions of the supporting frame. figure 3.7 is a model that was built for the supporting frame according to the sizes shown in Table 3.2.

**Table 3.2:** Specifications of support frame.

Dimension	Value (mm)
Length of the support frame (l)	2000
Breadth of the support frame (b)	700
Thickness of the support frame (t)	30

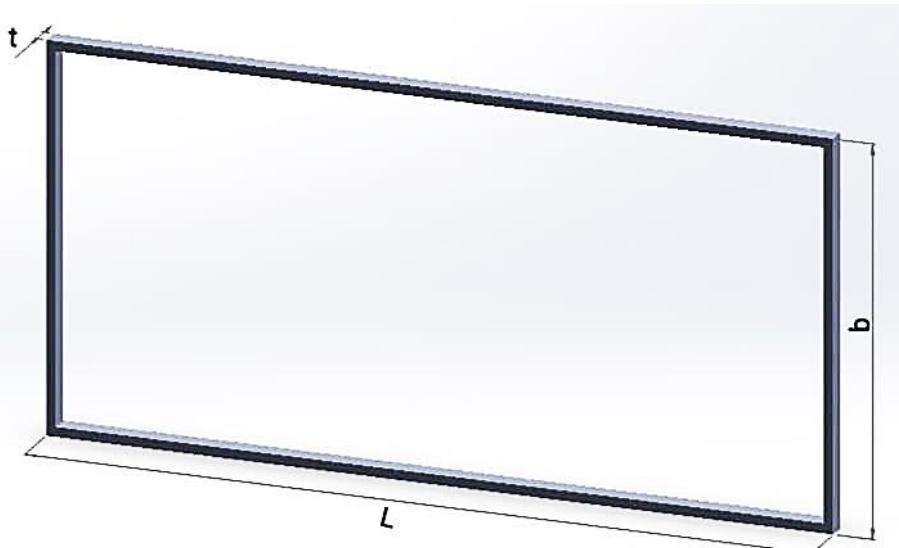


**Figure 3.7:** The supporting frame view.

### 3.2.3 Radiation Absorber Tube

It is a tube made of chrome due to its high ability to resist corrosion and rust and withstand high temperatures, as its melting temperature reaches 3400 °C. The tube length reaches 2200 mm, the outer diameter is 25 mm, and the inner diameter is 23 mm. The reflecting surface is centered and the amount of liquid (water) is placed inside it, where the sun's rays are directed towards it for the water to turn into steam, which in turn is used to produce electricity. The following table 3.3 shows the sizes of the radiation absorption tube. Figure 3.8 is a model of the tube that was constructed from chromium.

**Table 3.3:** Specifications of absorber tube.

Dimension	Value (mm)
Inner diameter of the tube ( $d_i$ )	23
Outer diameter of the tube ( $d_o$ )	25
Length of the tube ( $l$ )	2200

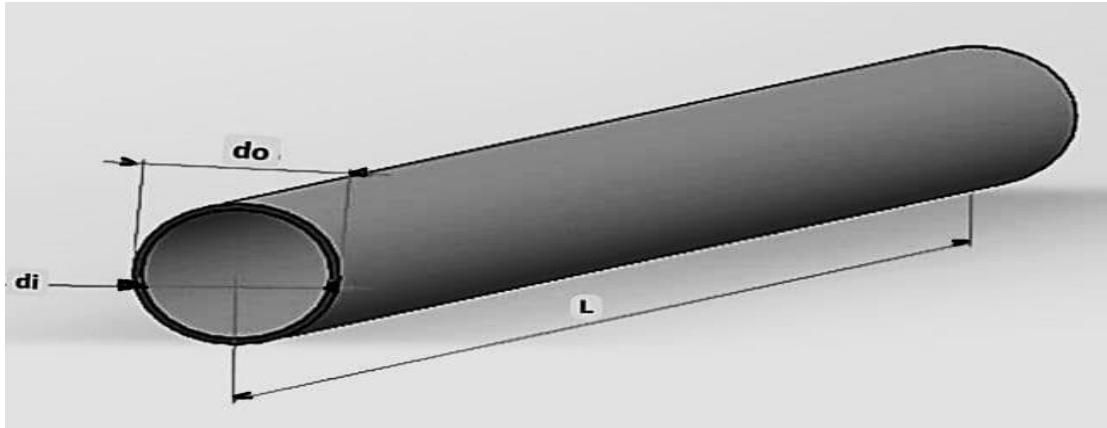


**Figure 3.8:** The radiation absorber tube view.

### 3.2.4 Parabolic Trough

The reflector is the part that absorbs sunlight and directs it to its center (tube) to obtain the desired dimensions and the ideal final reflection a highly polished aluminum plate was used and was bent in an arc. Table 3.4 shows the sizes of the parabolic trough. Figure 3.9 shows the sizes of the reflective surface of the solar collector, which was constructed of aluminum.

**Table 3.4:** Parabolic trough sizes.

Dimension	Value (mm)
The length of the reflector (L)	2000
The arc length of the reflector (W)	700
The arc radius (R)	500
Thickness of parabolic trough (t)	0.8

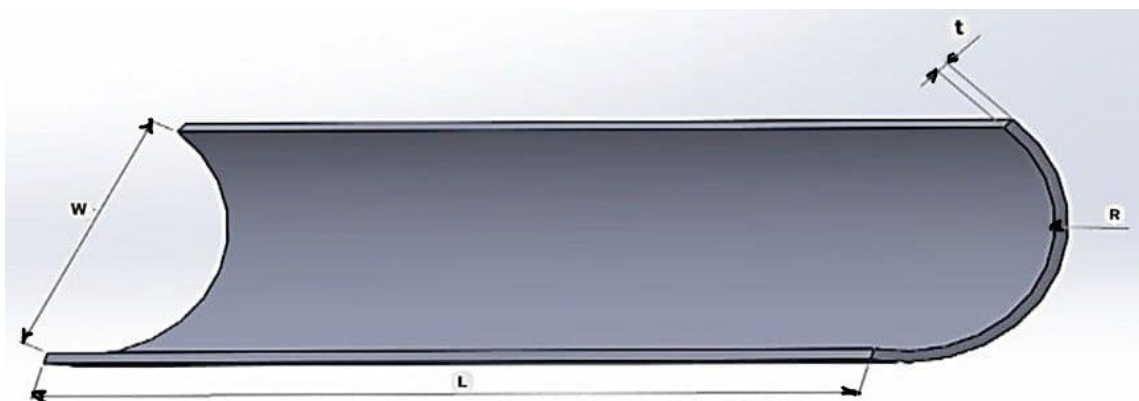


**Figure 3.9:** The parabolic trough view.

### 3.2.5 The Final Form of the Solar Collector

The solar collector, as mentioned in the previous steps, consists of the support holder, which carries the support frame at its top, and with it, the reflective surface that was built of aluminum is attached, and in the middle is an absorption tube made of good chromium and carries liquid (water) inside it. The solar collector collects the temperatures from the sun's rays during the day to be used in the production of steam needed in the production of clean thermal energy without polluting the environment or leaving residues, and this energy produced is converted by the electric generator into mechanical energy. The following figure 3.10 shows all parts of the solar collector together.



**Figure 3.10:** The solar energy collector view.

### 3.2.6 Solar Collector Efficiency

This section introduces the main parameters for the analysis. The thermal efficiency, available solar radiation, and use of energy are necessary for all calculations. Therefore, the energy that takes advantage of and the amount of efficiency of the solar collector can be determined to determine the ability of the complex to work under natural conditions and the amount of useful energy. The following equation (3.1) can be calculated the efficiency [4].

$$\eta_{co} = \frac{Q_u}{A_c \times H \times R} \quad (3.1)$$

Where  $\eta_{co}$  is the efficiency of the solar collector,  $Q_u$  is net useful heat gained by fluid,  $A_c$  is collector area,  $H$  is the average solar radiation and  $R$  is tilt factor for beam radiation. Since the net useful heat gained by the fluid can be calculated from the following equation (3.2).

$$Q_u = m \times c_p (T_{fo} - T_{fi}) \quad (3.2)$$

Where  $m$  is mass of fluid,  $c_p$  is specific heat capacity at constant pressure,  $T_{fi}$  is fluid inlet temperature and  $T_{fo}$  is fluid outlet temperature. The mass and collector fields are calculated from the following equations (3.3) and (3.4), respectively.

$$m = \rho \times v \quad (3.3)$$

$$A_c = \pi d^2/4 \quad (3.4)$$

Where  $\rho$  the density,  $v$  is the volume,  $A_c$  is collector area and  $d$  is the collector diameter [4].

### 3.2.7 Steam Flow Inside the Tubes

To measure the steam flow within the tubes, the area of the tube used is calculated, which can be obtained from the equation (3.5). The saturated vapor table at the optimum temperature that the solar collector has achieved, which is equal to, can also be used to determine the qualitative size of steam ( $v_g$ ) (143°C). The equation (3.6) can be used to calculate the volumetric flow rate.

$$A_{tube} = \pi r^2 \quad (3.5)$$

$$\dot{V}_g = \dot{v}_g \times \dot{m} \quad (3.6)$$

Where  $A_{tube}$  is the area of the tube,  $r$  is the radius of the tube,  $\dot{m}$  is the mass flow rate,  $\dot{v}_g$  is specific volume and  $\dot{V}_g$  is volumetric flow rate. Thus, equation (3.7) is used to calculate the vapor flow over time, and equation (3.8) is used to calculate the rate of vapor flow through the tube area [30].

$$Q = \frac{m \times (h_2 - h_1)}{t} \quad (3.7)$$

$$\dot{Q} = \frac{Q}{A} \quad (3.8)$$

Where  $Q$  is the vapor flow,  $m$  is the mass of fluid,  $h_2$  is the specific enthalpy at  $T_2 = 143$  °C,  $h_1$  is the specific enthalpy at  $T_1 = 40$  °C,  $\dot{Q}$  is the flow rate,  $A$  is the area of tube.

### 3.3 ELECTRICAL GENERATOR

The engines that are used at present to produce electricity are gasoline and diesel engines. These engines produce pollutants that are harmful to nature and the environment to a large extent, and because of them, they produce toxic chemicals and harmful to human health. In this thesis, the possibility of converting gasoline engines to steam-powered engines was studied in order to preserve the environment and produce electric energy at the lowest cost. To complete this process, it is necessary to refer to adjustments to the combustion chamber of the TIGER-TG3700E gasoline engine to be suitable for running on steam.

It should be noted here that the engine consists of a combustion chamber and an electric generator, which are the main parts responsible for producing mechanical and electrical kinetic energies. Table 3.5 shows the characteristics of the electric generator used and figure 3.11 illustrates the modified alternator used.

**Table 3.5:** The characteristics of TIGER-TG3700E generator [19].

Alternating current output	220 V
Direct current output	12 V
Current	8.3 A
Phase number	Single
Engine specifications	Thermal transfer 200, maximum predator 6.5 hours power, 2.5 kw, 4-stroke single cylinder, air cooled, overhead valve OHV
Generator	2-pole, self-exciting, synchronous, 100% copper Enameled wire
System startup	Electrician
Source of Energy	Petrol
Capacity of the Fuel Tank	12L
Dimensions (L×W×H)	525×460×460
Weight	45 Kgs
Runtime per Tank	12 Hrs



**Figure 3.11:** The TIGER-TG3700E generator view.

### 3.3.1 Design of Steam Engine

The mechanical energy production process in steam engines is as follows: the inlet valve opens and the steam enters directly into the combustion chamber where it pushes the piston from TDC to BDC, forming the first stroke. Then it produces the piston reaction force from the first movement that moves the piston from BDC to TDC. During the last operation, the exit valve is opened to expel the steam inside the engine cylinder. That is, the steam engine needs two cycles to complete one production process, the first half is the entry of steam and the second is the exit of steam from the engine [23].

In order for the gasoline four-stroke engine to be suitable for working on steam, the power production system must be changed during one cycle of the crankshaft. That is, in gasoline engines, mechanical kinetic energy is produced during four strokes, because the crankshaft contains a protrusion (metal protrusion) that opens each valve once during four strokes. As for steam engines, mechanical energy is produced through only two strokes. Therefore, it is necessary to work on the possibility of opening the inlet and outlet valves twice during these four strokes. In order to open the valves twice, a second protrusion is added in the opposite direction to the presence of the first protrusion so that the valves open every  $180^\circ$  of rotation of the camshaft, and this protrusion must be similar to the pre-existing protrusion.

Also, the presence of the spark is necessary in internal combustion engines because it is responsible for the formation of the explosion stroke, which is the main stroke in gasoline engines. As for steam engines, they are harmless and do not work here, so they are canceled. Figure 3.12 (a) shows the original design of the engine and the shape of the combustion chamber of gasoline engines, which consists of an inlet valve (through

which oxygenated gasoline enters the combustion chamber), a spark (helping to cause the explosion), a piston (responsible for producing mechanical kinetic energy) and an outlet valve that Throws out combustion residues after the explosion [23]. Figure 3.12 (b) is an illustrative diagram showing the combustion chamber after making the modification, and the shape of the camshaft after the change as well, that is, after it has been made suitable for working on steam.

As shown in the figure below, not much has been changed in the combustion chamber and there is no need to add a new material or manufacture, but merely modifying the working mechanism becomes suitable for working with steam instead of gasoline.

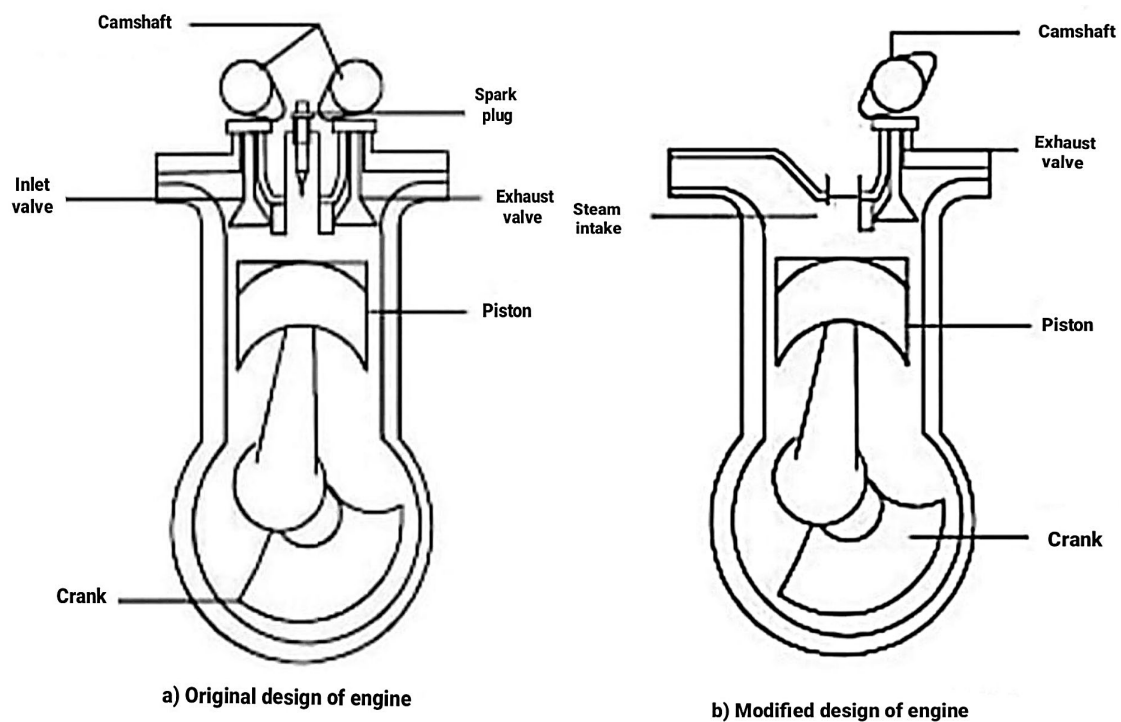


**Figure 3.12:** Schematic view of original (4-stroke) and modified (2-stroke) engines [23].

### 3.3.2 Engine Characteristics after Modification

The temperature of the steam generated by the solar collector was 143 °C and this heat is sufficient to generate a vapor pressure of up to 4 bar. In order to reduce the losses and losses that can occur to steam, it is not stored, but is sent directly to the engine through insulating tubes. That is, the steam enters the engine room with its qualities intact, such as a steam flow of 30.46 m<sup>3</sup>/h and a power of 166.106 N. As a result of this force, the engine may function at a high capacity of around 332.21 W.

Where steam enters, it causes the production of mechanical kinetic energy resulting from the movement of the garden inside the engine. This energy is utilized when it is converted into electrical energy, as the energy coming out of the engine has reached 774 J, and this is sufficient to produce a torque of 11.13 Nm. Through this torque, it is possible to know the horsepower of the engine resulting from this amount of steam, as the horsepower reached 1.59 HP and the engine capacity was 1.19 kW. As for the current generated by this motor, it has reached 2.4 A, and these values can be increased by increasing the used collectors.



**Figure 3.13:** The modified engine.

### 3.3.3 Calculations and Characteristics of Modified Engine

The modified engine has several good and acceptable characteristics compared to its operating cost and impact. These characteristics can be known by several laws that prove the possibility of its work.

#### 3.3.3.1 Volumetric flow rate

The volumetric flow rate of steam in the engine combustion chamber can be calculated by knowing the volume of steam by using the saturated steam table. Since the maximum temperature reached by the solar collector is 143 °C, it is possible to know the  $v_g$ , since at this temperature it is equal to (0.46242 m<sup>3</sup>/kg). The volumetric flow rate can be calculated from equation (3.9)

$$\dot{V}_g = v_g \times \dot{m} \quad (3.9)$$

### 3.3.3.2 Mass flow rate

The mass flow rate of steam inside the engine combustion chamber can be calculated by knowing the volumetric flow rate divided by the volume reached by the steam at a temperature of 143 °C. The mass flow rate is calculated from equation (3.10).

$$\dot{m} = \dot{V}_g / v_g \quad (3.10)$$

Where  $\dot{V}_g$  is the specific volume of liquid,  $v_g$  is the qualitative size,  $m$  is the mass of fluid and  $\dot{m}$  is the mass flow rate [30].

### 3.3.3.3 Work

The work done by the engine is calculated by the force multiplied by its arm. As in the equation 3.11. As for the energy coming out of the engine, it is calculated through the law of efficiency, where the energy out is equal to the energy in multiplied by the efficiency of the engine. Equation 3.12 is used to calculate the output power [31].

$$work\ done = F \times S \quad (3.11)$$

$$W_{output} = W_{input} \times \eta_{eng} \quad (3.12)$$

Where *work done* is the work done by the engine,  $F$  is the force due to pressure,  $S$  is the force arm  $W_{output}$  is the power output of the engine,  $W_{input}$  is the power input and  $\eta_{eng}$  is the efficiency of the engine.

### 3.3.3.4 Engine revolutions

It should be noted here that the number of piston cycles that were produced from the steam generated from a single solar collector with a square area of 2 m<sup>2</sup> can be calculated through the following equation (3.13)[32].

$$N = \frac{2 \times f \times 60}{P} \quad (3.13)$$

Where  $N$  the number of piston cycles is,  $f$  is the net frequency, and  $P$  is the number of poles.

### 3.3.3.5 Efficiency of engine

To know the success of the engine and the appropriate amount of output to obtain the electrical energy from the modified engine, it is necessary to calculate the efficiency of this engine and to calculate this efficiency first, the size of the combustion chamber must be known from the same height and diameter of the combustion chamber before the change because it has not been reduced or increased. Table 3.6 shows the engine specifications and thus the cylinder volume can be calculated from equation (3.13).

**Table 3.6:** Gasoline and steam Engine Specifications [33].

Name	Gasoline engine	Modified engine
Engine	TE200, 2.5 kW	TE150, 1.19 kW
Number of strokes	4-Stroke	2-stroke
Number of cylinders	Single	single
The length of the combustion chamber	85 mm	85 mm
The diameter of the combustion chamber	67 mm	67 mm
Engine revs	1000-1500 rpm	750 rpm
Source of Energy	Petrol	Steam
Emissions	Toxic emissions	No emissions

$$v_{cy} = \frac{\pi}{4} d^2 \times l \quad (3.13)$$

Where  $v_{cy}$  is the volume of cylinder,  $d$  is the cylinder diameter, and  $l$  is the length of cylinder, the engine's efficiency can be calculate from the equation (3.14) [28].

$$\eta_{en} = \eta_{carnot} \times \eta_{isent} \quad (3.14)$$

Where  $\eta_{carnot}$  is the expected Carnot efficiency and  $\eta_{isent}$  is the isentropic efficiency. The expected Carnot efficiency can be calculated from equation (3.15) [28].

$$\eta_{carnot} = \frac{T_{in} - T_{out}}{T_{in}} \quad (3.15)$$

Where  $T_{in}$  is the fluid inlet temperature and  $T_{out}$  is the fluid outlet temperature. If the steam expands within the cylinder, the effect is a decrease in temperature at the outlet

equal to the engine's power. A condenser was not included in the specification to reduce more system complexities and excessive capital expenditure for a basic water pumping system. The value of 55 °C is then chosen as a rational estimate of the engine's outlet steam temperature [28].

In this study, steam is transmitted directly from the solar collector to the engine through high temperature resistant rubber tubes. This is a study of how the two devices work together, and the results here are few, and this is normal because the area of the solar collector used is small, so the pressure and temperature are low. In order to operate this engine, a solar collector with an area of 8 m<sup>2</sup> must be used to collect temperatures up to 400 °C, and thus this heat generates a pressure of up to 15 bar. These are the values that this engine operates on. Figure 3.14 shows the engine with some modification.



**Figure 3.14:** Electric generator view after modification.

### **3.3.4 Design of Camshaft**

The camshaft used in small household electrical generators contains one lobe for each valve, which is responsible for opening the gasoline inlet valve and the combustion residue exit valve, and the valves are opened once within four strokes. Figure 3.15 shows the camshaft used in a four-stroke gasoline engine and figure 3.16 shows the vertical section for the camshaft to clarify the camshaft.

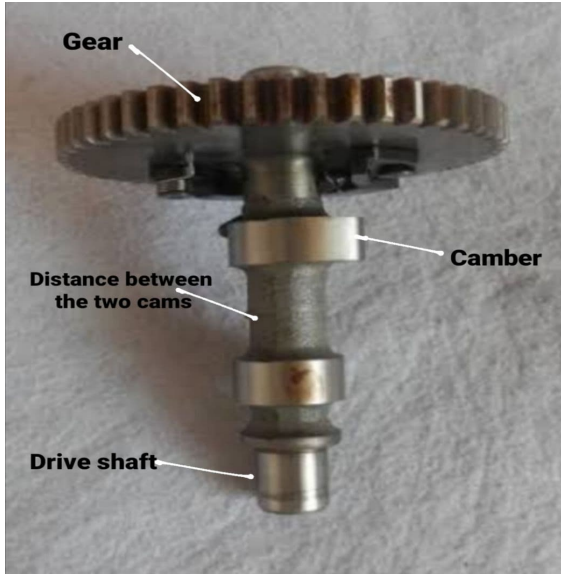


**Figure 3.15:** The view of the camshaft on the gasoline engine.

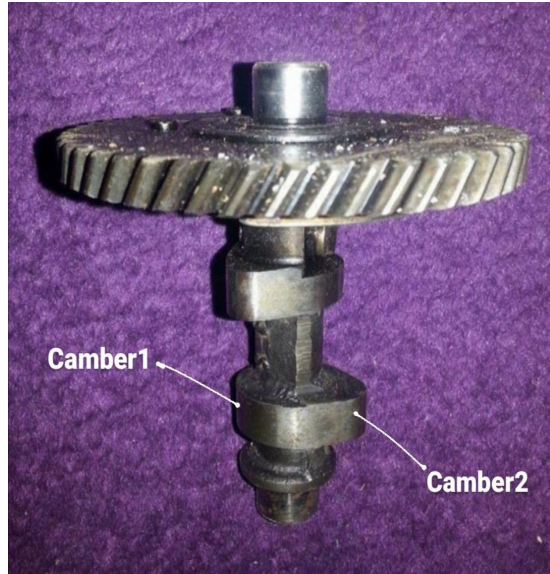


**Figure 3.16:** The view of the camshaft on the steam engine.

As for when converting the work of this engine to work on steam, it does not need four strokes, but only two strokes, which is the stroke of steam entry and its exit stroke. For this conversion to be done, a second lobe must be added, opposite to the direction of the first lobe, and thus the valve is opened twice instead of once. Figure 3.17 shows the camshaft after making a change to it to be suitable for two-stroke work on the steam generator figure 3.18 shows the vertical section of the camshaft added to the camshaft.

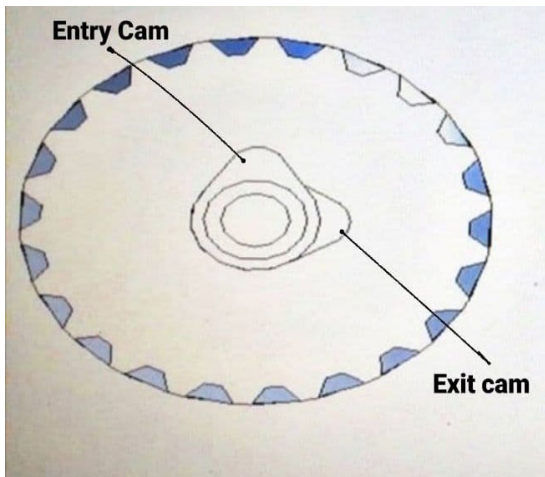


**Figure 3.17:** The vertical section of camshaft of the gasoline engine.

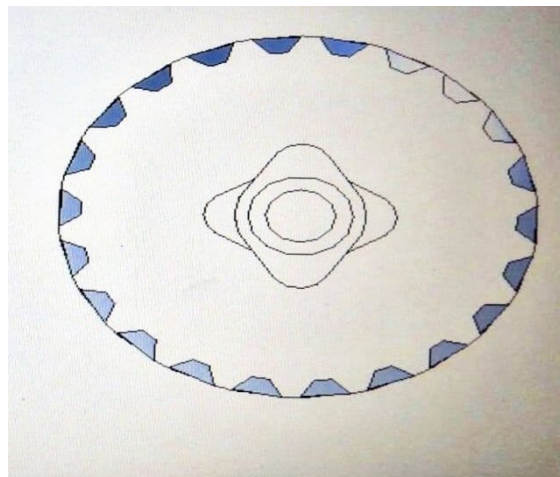


**Figure 3.18:** The vertical section of camshaft of the steam engine.

### 3.4 FINAL FORM OF THE EQUIPMENT

The electric power production line shown in this study is by collecting solar radiation from the first device. It is a solar collector with a parabola to convert the water inside the absorbent tube, which is located in the center of the collector, into steam. Then, the collected steam is sent to the second device, which is the modified engine. This device produces mechanical energy inside the engine and then converts it into electrical energy. It should be noted that the engine needs a solar collector with an area of 8 m<sup>2</sup> to create a pressure of 15 bar in order to run from solar energy. In the event that a collector with a large area such as 8 m<sup>2</sup> or more is used, a storage tank must be provided to collect steam inside it, because the area of the absorbent tube is not sufficient for the volume of steam generated. Figure 3.19 shows the devices used in this study with the location of the tank that can be used.



**Figure 3.19:** Final form of the equipment view.

## **4 RESULTS AND DISCUSSION**

### **4.1 CALCULATIONS**

What is important to know here knows the temperatures obtained during three weather conditions (wet, dry, and sunny) and knowing the pressure generated at this temperature. When these two readings are available, the solar collector efficiency and engine efficiency can be calculated, as well as the engine running time. Experiment test were carried out in dry and wet conditions on three separate days. The aluminum trough has been tested to assess the concentration of solar energy. With diagrams, the different outcomes were tabulated and evaluated.

### **4.2 WATER TEMPERATURE IN THE ABSORPTION TUBE**

To find out the amount of heat generated and produced from solar radiation, 3 days have been allocated to measure temperature and pressure. Provided that these days are varied for the weather and the purpose is to know the most efficient and productive weather. Choosing the best time when the temperatures are high and its purpose is to collect the largest amount of solar radiation, which is in the middle of the day between the hours of 1:00 PM to 3:30 PM. After displaying the solar collector on the rays of the sun, the temperature was measured using a thermometer and a pressure gauge with a manometer connected to the end of the absorbent tube after the first minute had passed from the solar collector display of the incident rays, then after 20 minutes had passed, it was measured again and after 40 minutes also the temperature and pressure generated were measured Thus, that is, every 20 minutes the readings are taken, and the purpose of it is to know the mechanism for increasing the readings, as these results were calculated at the University of Diyala / College of Engineering in Iraq. On days with variable weather it is (August 19, 2020, February 4, 2021, and March 3, 2021), the results were as follows:

#### **4.2.1 Data for the first day**

On the first day, it was chosen in moderate weather, with sunlight and light winds, and according to the specifications in Table 4.1 which shows the minimum and maximum temperature during the day and shows the amount of water used and the type of weather. Table 4.2 shows the results obtained during this day, represented by the temperature and the amount of pressure generated. These values were measured by a thermometer and the pressure was calculated by a manometer.

**Table 4.1:** Specifications of the first day.

First day	
Weather condition	Dry weather
Minimum temperature	30°C (around 1:00 PM)
Maximum temperature	120 °C (around 3:20 PM)
Amount of water	0.5 L

**Table 4.2:** Water test results in dry weather.

TIME	TEMPERATURE OF WATER(°C)	PRESSURE OF WATER (bar)
1:00 PM	30	0.5
1:20 PM	53	1.0
1:40 PM	65	1.7
2:00 PM	84	2.0
2:20 PM	92	2.6
2:40 PM	105	2.9
3:00 PM	117	3.2
3:20 PM	120	3.5

The results obtained from the solar collector and during the first day, where the weather is dry and the sunshine is high, were good and satisfactory to some extent, as a maximum temperature of 120 C° was obtained, and this temperature is good for obtaining a 3.5 bar water vapor pressure from a single compound of an area of 2 m<sup>2</sup>. The following figure 4.1 shows the process of changing the temperature during the time that amounted to two and a half hours, and it is clear that the temperatures during the first hour were low and normal, and then they reached the boiling point after an hour and a half.

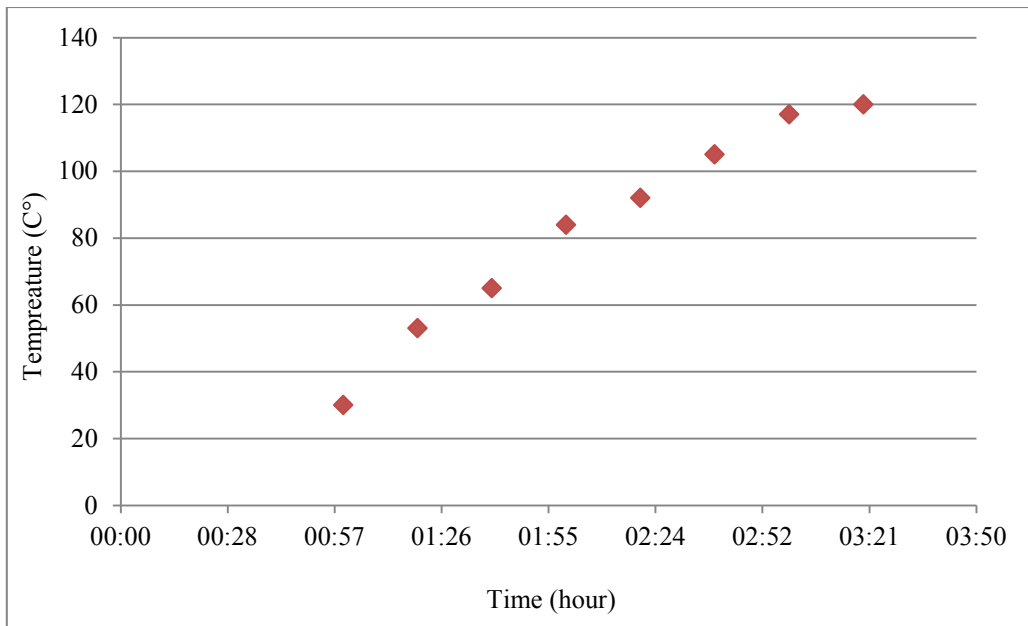


**Figure 4.1:** Change of water temperature according to time in dry weather conditions.

The temperature resulting from this complex is very high and dangerous, so safety reasons must be taken into account while dealing with it. Solar collectors must be placed in open and spacious places. As shown in the above figure, the temperature took more than an hour and forty minutes to reach 100 °C. This time depends on the amount of sunshine degrees, and after about two and a half hours, the temperature reached 120 °C. That is, if it becomes difficult to increase the accumulated temperature, and it remains in this state for a while. It turns out that the maximum temperature that can be collected during this weather and from this complex ranges between 120-130 °C.

But in case of increasing the collected temperature while reducing the time required to collect it, and must use a solar collector that is built in factories designated for this work, and using a reflective surface made of mirror, which is formed in the factory, and this requires a higher cost compared to the solar collector used in this study.

The following figure 4.2 shows the relationship between the pressure obtained from the solar collector and the time required to produce this pressure. As shown in this figure, the pressure is very weak in the first hour, as the water is still in its liquid state, but its temperature is high during the passage of time, and after two and a half hours, the water turns into steam. When the water completely turns into steam, it generates a high pressure and the pressure from this collector has reached 3.5 bar. This amount of pressure is not enough to start the engine, but it is good because from one solar collector it does not exceed its 2 m<sup>2</sup> area. In order for the electric motor to operate, a pressure of up to 15 bar must be provided, and this pressure is generated from a solar collector of an area of 8 m<sup>2</sup>, or the use of a solar collector with a reflective surface made of mirror that is formed in factories designated for this work in order to reflect more sunlight.

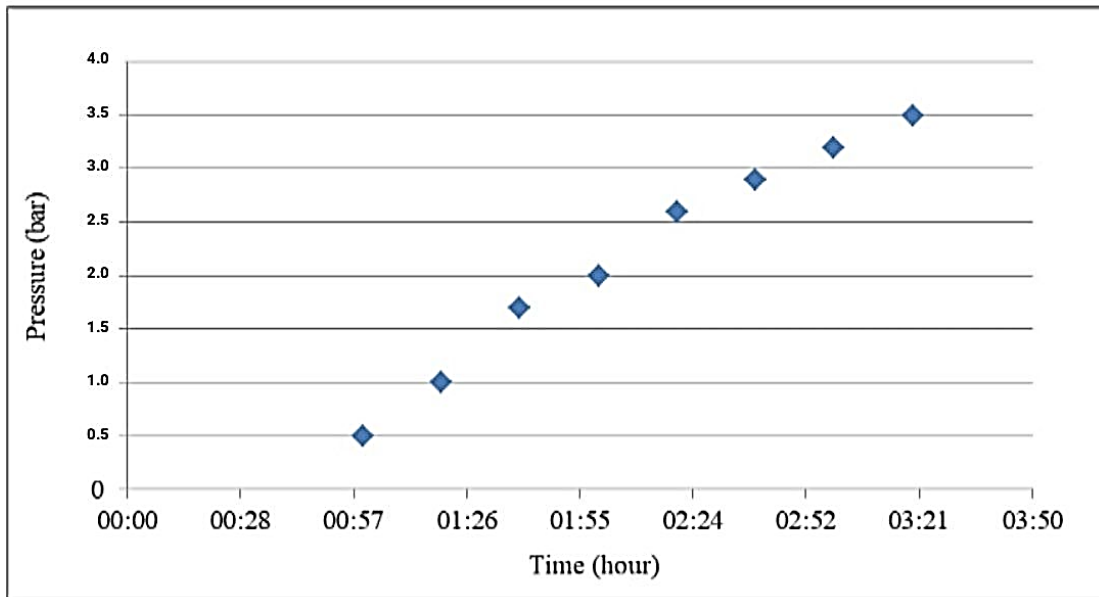


**Figure 4.2:** Change of water pressure according to time in dry weather conditions.

#### 4.2.2 Data for the second day

On the second day, it was chosen in wet weather, with sunlight and winds, and according to the specifications in Table 4.3 which shows the minimum and maximum temperature during the day and shows the amount of water used and the type of weather. Table 4.4 shows the results obtained during this day, represented by the temperature and the amount of pressure generated.

**Table 4.3:** Specifications of the second day.

Second day	
Weather condition	Wet weather
Minimum temperature	22 °C (around 1:00 PM)
Maximum temperature	85 °C (around 3:20 PM)
Amount of water	0.5 L

**Table 4.4:** Water test results in wet weather.

TIME	TEMPERATURE OF WATER (°C)	PRESSURE OF WATER (bar)
1:00 PM	22	0.0
1:20 PM	38	0.6
1:40 PM	50	1.1
2:00 PM	61	2.0
2:20 PM	78	2.5
2:40 PM	85	2.9
3:00 PM	81	2.9
3:20 PM	75	2.7

The results obtained from the solar collector and during the second day, where the humid weather and low sunlight were unsatisfactory and weak to some extent, as a maximum temperature of 85 C° was obtained, and this temperature is not good for obtaining high water vapor pressure and that the maximum pressure obtained was reached 2.9 bar from a single complex has an area of 2 m<sup>2</sup>. The following figure 4.3 shows the process of changing the temperature during the time that amounted to two and a half hours, and it is clear that the temperatures during the first hour were low and normal, then after an hour and a half the resulting temperature did not reach the boiling point and the water was kept in a liquid state and was satisfied with a high temperature with little evaporation.

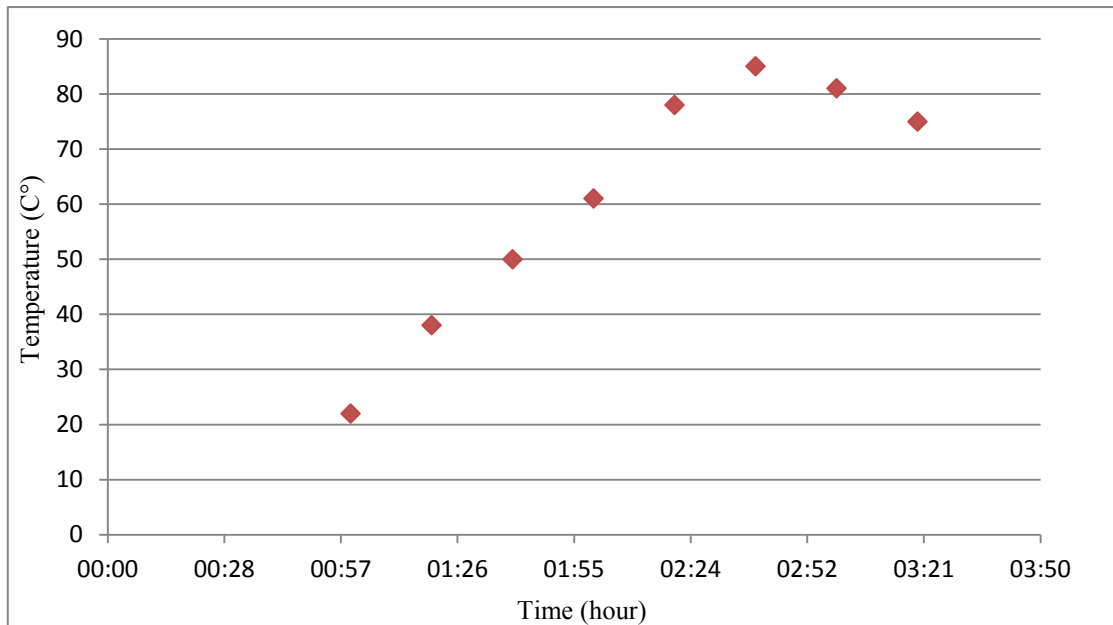


**Figure 4.3:** Change of water temperature according to time in wet weather conditions.

To increase the temperature under these conditions, it is necessary to use a reflective surface made of mirror with good reflection, or to increase the area of the reflective surface in order to collect a temperature of up to 100 °C.

The following figure shows the relationship between the pressure that was obtained on the second day of the solar collector and the time that was required to produce this pressure, and as shown in the following figure 4.4 that the pressure is very weak in the first hour as the water is still in the liquid state but its temperature is high after two and a half hours part of the water turned into steam and the other part remained liquid while maintaining its high temperature, and this caused a low pressure, which reached 2.9 bar. This amount of pressure is insufficient to start the engine and is weak because it is from one solar complex that does not exceed its square area of 2 m<sup>2</sup> during wet weather.

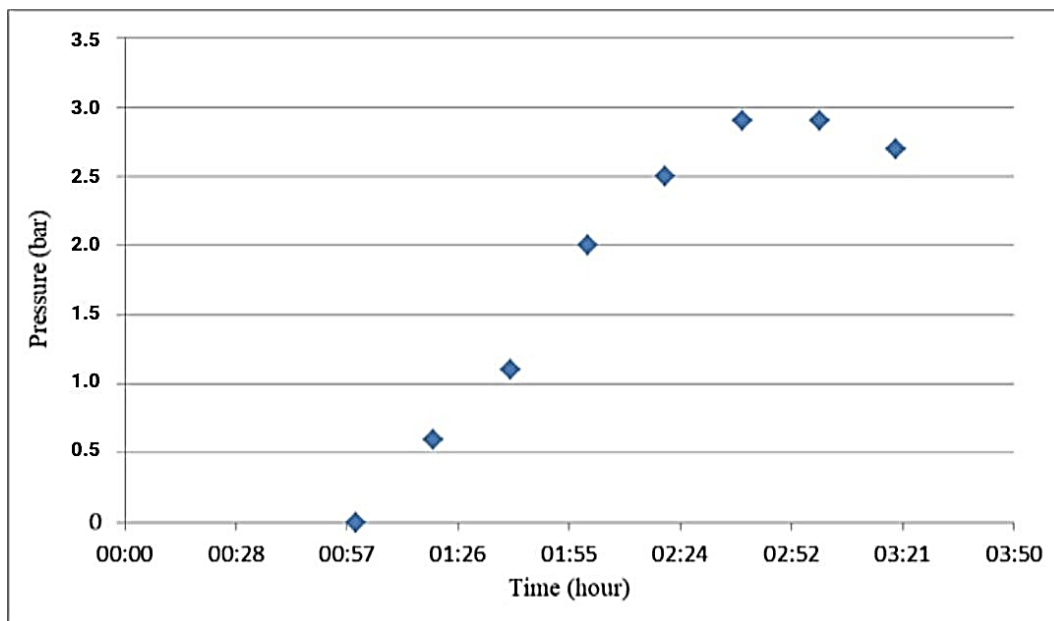


**Figure 4.4:** Change of water pressure according to time in wet weather conditions.

#### 4.2.3 Data for the third day

On the third day, it was chosen in sunny weather, with strong sunlight, and without winds. And according to the specifications in table 4.5 which shows the minimum and maximum temperature during the day and shows the amount of water used and the type of weather. Table 4.6 shows the results obtained during this day, represented by the temperature and the amount of pressure generated. These values were calculated by a thermometer and the pressure was calculated by a manometer.

**Table 4.5:** Specifications of the third day.

Third day	
Weather condition	Sunny weather
Minimum temperature	40°C (around 1:00 PM)
Maximum temperature	143 °C (around 3:20 PM)
Amount of water	0.5 L

**Table 4.6:** Sunny weather test results.

TIME	TEMPERATURE OF WATER (°C)	PRESSURE OF WATER (bar)
1:00 PM	40	0.1
1:20 PM	65	1.7
1:40 PM	90	2.3
2:00 PM	110	2.8
2:20 PM	122	3.1
2:40 PM	130	3.4
3:00 PM	138	3.8
3:20 PM	143	4.0

The results obtained from the solar collector during the third day, Where the sunny weather and strong sunlight were very satisfactory, high and with an excellent result. Where a maximum temperature of 143 °C was obtained and this temperature is good for obtaining a high water vapor pressure and the maximum pressure was obtained it amounted to 4.0 bar from a single complex with an area of 2 m<sup>2</sup>. The following figure 4.5 shows the process of changing the temperature during the time that amounted to two and a half hours. And it is clear that the temperatures are high, as it reached the boiling temperature during the first hour only, then after two and a half hours after the start of the temperature calculation, the temperature reached 143 °C and the pressure reached 4 bar, which means that the water turned fully compressed into highly compressed steam.

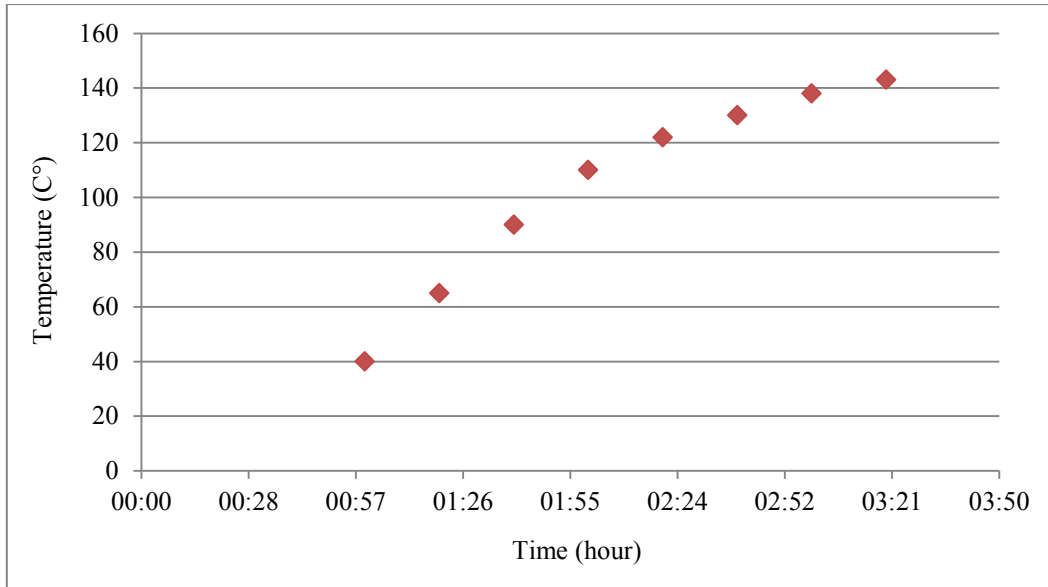


**Figure 4.5:** Change of water temperature according to time in sunny weather conditions.

The following figure 4.6 shows the relationship between the pressure that was obtained on the third day of the solar collector and the time that was required to produce this pressure. The cold liquid to boiling and the start of the transformation into a gaseous state and after two and a half hours passed it completely transformed into high-pressure steam, where the pressure reached 4.0 bar. Figure 4.6 below also shows the stages of this liquid's transformation from a liquid state to a gaseous state during the time from a single solar collector that does not exceed its square area of 2 m<sup>2</sup> and during sunny weather.

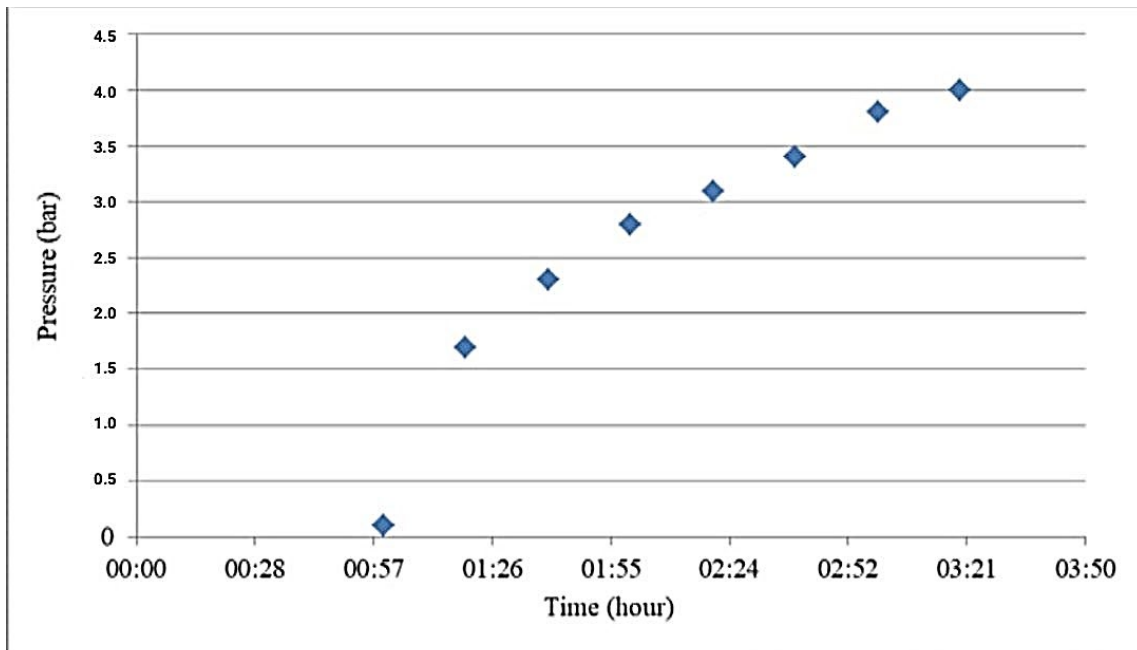


**Figure 4.6:** Change of water pressure according to time in sunny weather conditions.

### 4.3 COMPARING THE SOLAR COLLECTOR TO ANOTHER COLLECTOR

A parabolic-shaped solar collector was designed similar to the one used in this study, the researcher used a 2 m<sup>2</sup> collector to collect sunlight temperatures. Here, the researcher was able to collect temperatures from a full day around 80 to 145 °C with the addition of a sun tracker. That is, the collector is directed towards the sun's rays and water is placed inside the absorbent tube to be heated and converted into steam. The time it took for this complex to reach the temperature of 145 °C about 7 hours, and the amount of water used is 750 cm<sup>3</sup>, with mass 0.75 kg. And under a solar flow rate of 250-780 W/m<sup>2</sup>. The researcher found that at a cumulative temperature of 145 °C and the pressure generated between 2.7 and 15 bar during a whole day, the enthalpy of evaporation was about 2720.8 kJ / kg, and the efficiency of the solar collector was about 58.94 %, and during a whole day the efficiency of the collector did not exceed 60 %. The researcher also indicated that cylindrical solar collectors with a flexible surface are better. Figure 4.8 illustrates the use of a parabolic trough solar collector made of a reflective mirror to collect temperatures [30], [34].



**Figure 4.7:** Parabolic solar collector view.

In this study, a 2 m<sup>2</sup> cylindrical solar collector was used and some modifications were made to it, such as the use of aluminum foil adhered to a molded flexible surface to ensure the best reflection of sunlight. At an average solar flux of 290-830 W/m<sup>2</sup>, sunlight falling on the collector was reflected toward the center of focus where the tube contained a pint of water. Within two and a half hours, the temperature reached between 80 °C and 143 °C and this temperature gives a pressure of up to 4 bar during sunny weather. The efficiency of the solar collector was 65.98 %. And when using the same conditions that were worked on in the solar heat was collected for a longer period of time, for example for 7 hours, the results would have been good and much more, but the goal here is to collect high heat in less time. Figure 4.7 shows the efficiency of the solar collector used in this study with another solar collector during different weather.

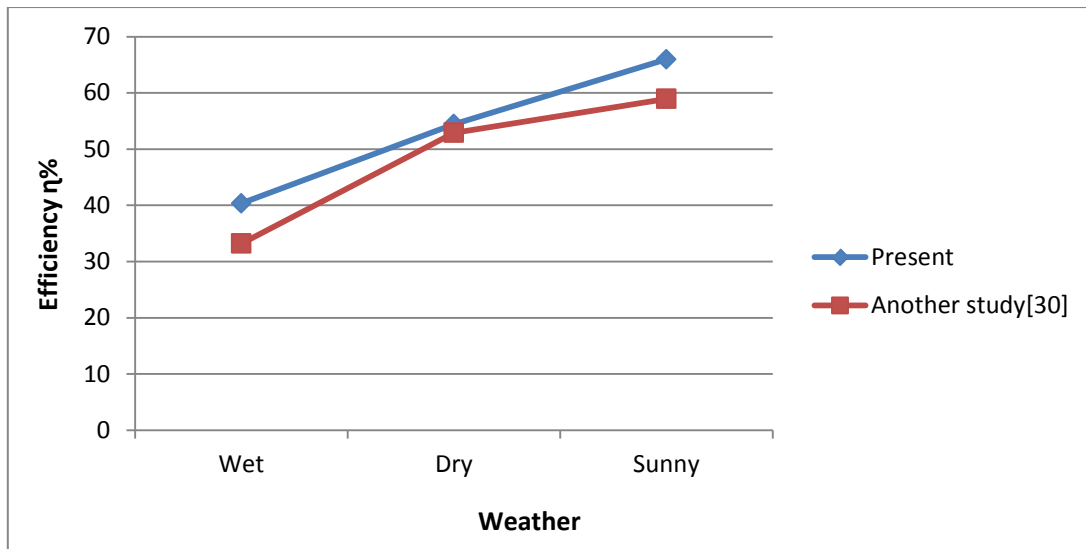


**Figure 4.8:** Comparing the efficiency of the modified solar collector with the efficiency of its predecessor.

#### 4.4 DISCUSS THE CALCULATION OF SOLAR COLLECTOR EFFICIENCY

The calculation of the operating efficiency of the solar collector is necessary to know the extent to which thermal energy can be saved during work and the extent of benefit from this device. This efficiency is calculated through equation (3.1) which is the net useful heat gained by fluid ( $Q_u$ ) divided by the collector area ( $A_c$ ), the average radiation solar ( $H$ ), and the Tilt factor for radiation ( $R$ ). As the value of ( $Q_u$ ) can be found from equation (3.2) and the area of the solar collector was found from equation (3.4). The resulting values are as shown in the following table 4.7.

**Table 4.7:** Results of solar collector efficiency and net useful heat gained values.

Dry weather		Wet weather		Sunny weather	
$Q_u (W/m^2)$	$\eta_{col}(\%)$	$Q_u (W/m^2)$	$\eta_{col}(\%)$	$Q_u (W/m^2)$	$\eta_{col}(\%)$
177.65	54.45	131.67	40.36 %	215.27	65.98 %

The above results illustrate the above showing the value of the net useful heat gained by fluid as its value in sunny weather is very high and reached  $215.27 \text{ W / m}^2$  as it reached its highest levels on this day because the solar radiation is high and since the net useful heat gained by fluid peak depends on the maximum and minimum temperatures, it increases as The solar heat increased, and for this, it was found that the efficiency of the solar collector is high on a sunny day, and the highest efficiency was obtained, reaching 65.98 %. This is in contrast to what was obtained on a wet day as the net useful heat gained by fluid value was at the lowest level of  $131.67 \text{ W / m}^2$  due to the weak radiation

The low temperatures produced during this day are due to the winds and clouds that block the rays of the sun to reach the earth is weak. Therefore, the efficiency value was observed that was weak compared to other weather, as the efficiency of the solar collector in wet weather reached about 40.36 %, which is very weak.

From here, the effectiveness of the solar collector was deduced, and this efficiency can be increased in several ways, such as using a reflective mirror to ensure maximum reflection of the falling rays of the sun. Also, the solar collector basin can be covered with a glass plate to prevent the dispersion of solar rays and reduce thermal losses.

#### 4.5 COMPARISON OF A MODIFIED STEAM ENGINE TO AN ORIGINAL ONE

In a previous study entitled design and characterizations of solar steam engine, the researcher converted a single-cylinder engine and made it suitable for working on steam, as this engine works on steam coming from the boiler, which heats the water and turns it into steam at a temperature of 150 °C and a steam pressure of 15 bar. The Carnot efficiency was about 19.8 % and the efficiency of the steam engine was 9.5 %. Figure 4.2 shows the steam engine used by the researcher [28].

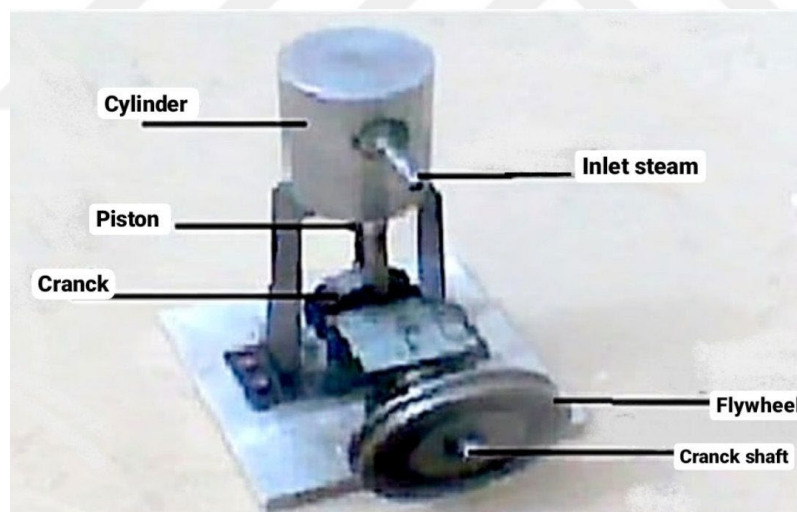


**Figure 4.9:** steam engine view [28].

In this study, a four-stroke household engine was converted into a two-stroke engine running on steam. The camshaft has been modified by adding a cam opposite to the old cam responsible for opening and closing the valves, and through this new camshaft, the valves opened twice within four strokes. After it started the engine, it was found that the efficiency of the Carnot reached 21.2 % and the efficiency of the steam engine reached 10.6 %, and this is within two and a half hours of the solar collector being run on it during sunny weather. Table 4.8 shows the differences between the modified engine used in this study and another engine.

**Table 4.8:** The differences between modified engine and another engine [35].

Sympathies	4- stroke engine	Steam engine
Mean effective pressure (kPa)	3200	1500
Energy power (kW)	2.5	1.19 (at 4 bar)
Horsepower (hp)	6.5	1.59
Cost of engine \$	150	It can be produced by modifying a four-wheel drive consumable at a cost of up to 50\$.
Ignition degree (°C)	450-550	300-400
Efficiency %	22 - 28	10 - 13

#### **4.6 RESULTS AND DISCUSSION OF THE MODIFIED ENGINE**

The calculation of engine efficiency is necessary to know that the engine can run on steam only and without combustion. As the engine efficiency was calculated from equation (3.12), which is based on the value of the expected Carnot efficiency and the isentropic efficiency where the expected Carnot efficiency is found from equation (3.13). As for the value of the isentropic efficiency, if the steam expands within the cylinder, the effect is a decrease in temperature at the outlet equal to the engine's power. A condenser was not included in the specification to reduce more system complexities and excessive capital expenditure for a basic water pumping system. The value of 55 °C is then chosen as a rational estimate of the engine's outlet steam temperature. Besides, small-scale steam engines of this type usually lack substantial regenerators and reheaters and, as a consequence, typically have approximately poor isentropic efficiencies 50 %. For the same inlet state and exit pressure, the isentropic efficiency requires a distinction between the current performance of a system and the performance that obtained under ideal conditions. The values of these competencies were obtained as shown in Table 4.9.

**Table 4.9:** Efficiency values of the modified engine.

Dry weather		Wet weather		Sunny weather	
$\eta_{carnot}$	$\eta_{eng}$	$\eta_{carnot}$	$\eta_{eng}$	$\eta_{carnot}$	$\eta_{eng}$
16.5 %	8.25 %	8.4 %	4.2 %	21.2 %	10.6 %

The results obtained are excellent compared to the size of the small engine and the amount of heat used from one small solar collector. Whereas, when the area of the solar collector increases and the size of the engine increase, the efficiency increases. This is shown in Table 4.9 above, as the higher the temperature, as in sunny weather, the greater the value of the expected Carnot efficiency, and thus the efficiency of the electric motor increases. The lower the temperatures produced by the solar collector, the lower the efficiency, as in wet weather.

It is also possible to know the number of revolutions that the piston rotates and that result from the combustion chamber through equation (3.14), as this number of revolutions is a specific volume divided by the volume of the combustion chamber. As the highest value of the number of cycles reached 750 rpm cycles from this collector, and this value can be increased by increasing the number of collectors used to collect solar radiation, as the number of collectors used is multiplied by 750 rpm. The calculation of the number of cycles is used to know the value of the electric current produced by this device.

A revolution count of 750 rpm was obtained, and these values can be increased by using a solar collector with a larger area. Since if a solar collector with an area of 4 m<sup>2</sup> is used, the number of cycles is 1500 rpm, and this is an excellent value that can be used and good electrical energy produced from it. The steam flow rate reached 30.46 m<sup>3</sup>/h and the engine power was 1.19 kW from one collector. The output power of the engine is 774 J. As for the current generated by this motor, it has reached 2.4 A, and these values can be increased by increasing the used collectors. These values are good compared to the area of the solar collector used.

#### **4.7 SOLAR COLLECTOR TEMPERATURE RESULTS**

Through the above results obtained from one solar collector and steam engine, concluded that the higher the weather temperature, the greater the liquid (water) temperature value, and consequently the vapor pressure value increases, and this value is the most important in obtaining a greater number of cycles the engine. On the first day when the weather was dry and at 30 °C, a steam temperature of 150 °C and a pressure of 3.5 bar were obtained. On the second day, when the weather was wet during the air temperature of 22 °C, a steam temperature of 85 °C and a pressure of 2.9 bar were

obtained. On the third day, it was sunny, and during 40 °C the steam temperature was 143 °C and the pressure was 4 bar. These results were obtained through the use of a solar collector at the College of Engineering at the University of Diyala - Iraq after making some modifications to it to give better results, then it was connected to the axis of the steam electric motor through resistance tubes and then increased temperatures. The two devices can work together to obtain electricity from solar energy during the construction of solar collectors on a large area in areas with high solar radiation.

#### **4.8 THE FINANCIAL COST AND FUTURE OUTLOOK**

The prospect of minimizing losses when generating electrical energy, saving labor and fuel, and not harming the environment leads one to consider solar energy and the steam generator, since the complexes do not need frequent maintenance, but rather manual cleaning of the dust accumulated on the inverter's surface, as well as follow-up on the generator and the addition of a solar tracking system. It's also possible to reuse modified and modified generators rather than creating them from scratch, which saves money. When the sun's rays are blocked, the produced current can be stored in batteries and used at night.

This study suggests that this approach should be used for the time being because it does not harden much and is inexpensive. Built for only \$150, a 1,000 square meter solar collector can be built for less than \$10,000 and last more than 50 years if properly maintained. These manifolds can collect temperatures that maintain high pressure generation to keep the engine running and not shutting down every day. This approximation means that the steam engine running for long periods of time. This has reduced the ongoing financial waste associated with the purchase of fuel for electric combustion generators, as well as the necessary periodic maintenance, all while protecting the environment and human health.

## 5. CONCLUSIONS AND RECOMMENDATIONS

### 5.1 CONCLUSIONS

Nowadays the need for energy is constantly increasing and traditional resources are being used at an alarming rate, hence there is an urgent need for alternative fuels. The technique of using steam engines can be one of the best alternatives, as the pollution produced is small, because the work products are steam as well, which is not harmful. It is also cost-effective as it can be manufactured to convert the work of a spent or semi-efficient combustion engine. Solar radiation is an abundant and free form of energy that can be directly converted or concentrated to generate energy. A literature review of the concentrating solar collector steam engine modified combustion engine was presented.

The results of this study proved the possibility of running the motor on solar collectors, as the efficiency of the solar collector was 65.98 %. It was obtained on a sunny day and using a solar collector with a reflective surface consisting of polished aluminum foil with an area of 2 m<sup>2</sup> and a water mass of not more than 0.165 kg with a time period of no more than two and a half hours after this efficiency was not more than 40.36 % using a reflective surface under the same Circumstances. As for the efficiency of the axial steam engine, it reached 10.6 % after it was only 9.5 % in previous experiments. The number of cycles of 750 rpm was obtained, and these values can be increased by using the solar collector with a larger area. The steam flow rate was 30.46m<sup>3</sup>/h and the engine power reached 1.19 kW. As for the current generated by this motor, it has reached 2.4 A, and these values can be increased by increasing the used collectors. The power output from the engine was 774 J. These values are good compared to the area of the collector used and the mass of water, which does not exceed 0.165 kg.

## 5.2 RECOMMENDATIONS FOR FUTURE WORK

The device can be improved in several ways:

- i. Using solar collectors of large areas to produce high temperatures sufficient to produce more electrical energy.
- ii. Swapping the sides of the solar collector with a mirror and attaching a solar tracking device.
- iii. The use of ceramic material in the manufacture of camshaft to reduce the effort exerted to open and close the valves, as well as making ceramic piston to reduce the effort spent in moving it and thus achieve the most benefit from the steam.
- iv. The use of large steam engines with solar collectors with a large area to produce more energy. Lithium batteries can be used to store energy and use it in times of sunlight outage.



## REFERENCES

- [1] M. J. Montes, A. Abánades, J. M. Martínez-Val, and M. Valdés, “Solar multiple optimization for a solar-only thermal power plant, using oil as heat transfer fluid in the parabolic trough collectors,” *Sol. Energy*, vol. 83, no. 12, pp. 2165–2176, 2009, doi: 10.1016/j.solener.2009.08.010.
- [2] E. Bellos, C. Tzivanidis, and K. A. Antonopoulos, “A detailed working fluid investigation for solar parabolic trough collectors,” *Appl. Therm. Eng.*, vol. 114, pp. 374–386, 2017, doi: 10.1016/j.applthermaleng.2016.11.201.
- [3] A. Fernández-García, E. Zarza, L. Valenzuela, and M. Pérez, “Parabolic-trough solar collectors and their applications,” *Renew. Sustain. Energy Rev.*, vol. 14, no. 7, pp. 1695–1721, 2010, doi: 10.1016/j.rser.2010.03.012.
- [4] V. R. 1 Pradeep Kumar K V1\*, Srinath T2, “INTERNATIONAL JOURNAL OF RESEARCH IN Design , Fabrication and Experimental Testing of Solar Parabolic Trough Collectors with Automated Tracking Mechanismradeep Kumar K Srinath, T Reddy, Venkatesh,” vol. 1, no. 4, pp. 37–55, 2013.
- [5] M. Karvonen, R. Kapoor, A. Uusitalo, and V. Ojanen, “Technology competition in the internal combustion engine waste heat recovery: A patent landscape analysis,” *J. Clean. Prod.*, vol. 112, pp. 3735–3743, 2016, doi: 10.1016/j.jclepro.2015.06.031.
- [6] R. Forristall, “Heat Transfer Analysis and Modeling of a Parabolic Trough Solar Receiver Implemented in Engineering Equation Solver,” no. October, p. 164, 2003, doi: NREL/TP-550-34169.
- [7] M. J. Montes, A. Rovira, M. Muñoz, and J. M. Martínez-Val, “Performance analysis of an Integrated Solar Combined Cycle using Direct Steam Generation in parabolic trough collectors,” *Appl. Energy*, vol. 88, no. 9, pp. 3228–3238, 2011, doi: 10.1016/j.apenergy.2011.03.038.
- [8] E. Bellos, C. Tzivanidis, K. A. Antonopoulos, and G. Gkinis, “Thermal enhancement of solar parabolic trough collectors by using nanofluids and converging-diverging absorber tube,” *Renew. Energy*, vol. 94, pp. 213–222, 2016, doi: 10.1016/j.renene.2016.03.062.
- [9] Z. Tian, B. Perers, S. Furbo, and J. Fan, “Thermo-economic optimization of a hybrid solar district heating plant with flat plate collectors and parabolic trough collectors in series,” *Energy Convers. Manag.*, vol. 165, no. October 2017, pp. 92–101, 2018, doi: 10.1016/j.enconman.2018.03.034.
- [10] A. Der Minassians, “Stirling Engines for Low-Temperature Solar-Thermal-Electric Power Generation,” p. 138, 2007, [Online]. Available:

<http://www.eecs.berkeley.edu/Pubs/TechRpts/2007/EECS-2007-172.html>.

- [11] X. zhi Li, Z. de Liu, H. chuan Li, Y. tian Wang, and B. Li, “Investigations on the behavior of laser cladding Ni-Cr-Mo alloy coating on TP347H stainless steel tube in HCl rich environment,” *Surf. Coatings Technol.*, vol. 232, pp. 627–639, 2013, doi: 10.1016/j.surfcoat.2013.06.048.
- [12] A. A. Minea and W. M. El-Maghlany, “Influence of hybrid nanofluids on the performance of parabolic trough collectors in solar thermal systems: Recent findings and numerical comparison,” *Renew. Energy*, vol. 120, pp. 350–364, 2018, doi: 10.1016/j.renene.2017.12.093.
- [13] W. W. Pulkrabek, “Engineering Fundamentals of the Internal Combustion Engine,” *J. Chem. Inf. Model.*, vol. 53, no. 9, pp. 1689–1699, 2013.
- [14] R. D. Reitz *et al.*, “IJER editorial: The future of the internal combustion engine,” *Int. J. Engine Res.*, vol. 21, no. 1, pp. 3–10, 2020, doi: 10.1177/1468087419877990.
- [15] I. C. Engine, E. C. Engine, I. C. Engine, B. D. Centre, and S. I. Engine, “Internal Combustion Engine : Spark-ignition engine : Compression ignition engine :”
- [16] R. Cristóvão, C. Botelho, R. Martins, and R. Boaventura, “Pollution prevention and wastewater treatment in fish canning industries of Northern Portugal,” *Int. Proc. Chem. Biol. Environ. Eng.*, vol. 32, no. 1, pp. 12–16, 2012, doi: 10.7763/IPCBE.
- [17] M. A. Afsar, A. M. Mahalle, and G. Polytechnic, “Analysis of Scavenging Parameters in Two Stroke Engine,” vol. 7, no. 2, pp. 1–8, 2018.
- [18] B. Bhamwala, R. Gopalachari, K. Kotak, and Y. Ramnani, “Design and Development of Air Powered Reciprocating Two Stroke Engine,” vol. II, no. Xi, pp. 1–4, 2015, [Online]. Available: [www.rsisinternational.org](http://www.rsisinternational.org).
- [19] “\_bct\_generateurs\_generators.pdf.” p. 14, 2012.
- [20] S. C. Crosbie, M. D. Polanka, P. J. Litke, and J. L. Hoke, “Increasing reliability of a small 2-stroke internal combustion engine for dynamically changing altitudes,” *50th AIAA Aerosp. Sci. Meet. Incl. New Horizons Forum Aerosp. Expo.*, no. January, pp. 1–12, 2012, doi: 10.2514/6.2012-950.
- [21] E. Mattarelli, G. Cantore, C. A. Rinaldini, and T. Savioli, “Combustion System Development of an Opposed Piston 2-Stroke Diesel Engine,” *Energy Procedia*, vol. 126, pp. 1003–1010, 2017, doi: 10.1016/j.egypro.2017.08.268.
- [22] M. Shahbaz A, M. Amir A, M. Mobasshir A, and V. Singh A A, “Sunlight Powered Steam Engine,” *Int. J. Curr. Eng. Technol. Gen. Artic. Int. J. Curr. Eng. Technol. E*, vol. 44, no. 33, pp. 2277–4106, 2014, [Online]. Available:

<http://inpressco.com/category/ijcet>.

- [23] A. Mourya, A. Khan, D. Bajpayee, and N. Gupta, “Modified Compressed Air Engine Two stroke engine working on the design of a four stroke petrol engine,” *Int. J. Theor. Appl. Res. Mech. Eng.*, no. 4, pp. 58–60, 2014.
- [24] G. Ferrara, G. Manfrida, and A. Pescioni, “Model of a small steam engine for renewable domestic CHP (combined heat and power) system,” *Energy*, vol. 58, pp. 78–85, 2013, doi: 10.1016/j.energy.2013.03.035.
- [25] S. SURESH, “History of the Four Stroke Autom mobile Engine,” (*M. TECH. Manuf. Ind. Eng. ) (Suresh Gy Gyan Vihar Univ. y, Jagatpura, Jaipur)*, 2010.
- [26] F. J. Espadafor, J. B. Villanueva, and M. T. García, “Analysis of a diesel generator crankshaft failure,” *Eng. Fail. Anal.*, vol. 16, no. 7, pp. 2333–2341, 2009, doi: 10.1016/j.engfailanal.2009.03.019.
- [27] M. S. K. P. Jeevanandha, M. Ganesh Prasanth, M. Rajesh, S. Santhos, “International Journal of Research in Aeronautical and Mechanical Engineering Heat Transfer Analysis on Shell and Tube Heat,” *Int. J. Res. Aeronaut. Mech. Eng.*, vol. 2, no. 1, pp. 11–26, 2014.
- [28] F. Mohamed, A. Jassim, Y. Mahmood, and M. Ahmed, “Design and Characterizations of Solar Steam Engine,” *Ijrrr.Com*, vol. IV, no. December, pp. 3–9, 2012, [Online]. Available: <http://www.ijrrr.com/papers4/paper1.pdf>.
- [29] S. Bhattacharya, A. Basu, S. Chowdhury and Y.S. Upadhyaya “Analysis of Piston of Two Stroke Engine,” *Int. J. Res. Eng. Technol.*, vol. 03, no. 06, pp. 642–648, 2014, doi: 10.15623/ijret.2014.0306119.
- [30] S. Shinde, R. Shinde, A. Patil, C. Desale, and M. Engineering, “Steam Generation by Using Solar Dish Collector,” *Int. Res. J. Eng. Technol.*, vol. 4, no. 6, pp. 4–7, 2017, [Online]. Available: <https://irjet.net/archives/V4/i6/IRJET-V4I679.pdf>.
- [31] M. El-Dairi and R. J. House, “Optic nerve hypoplasia,” *Handbook of Pediatric Retinal OCT and the Eye-Brain Connection*. pp. 285–287, 2019, doi: 10.1016/B978-0-323-60984-5.00062-7.
- [32] R. T. Sataloff, M. M. Johns, and K. M. Kost, *International Steam Tables*. 2008.
- [33] R. Cataluña, R. da Silva, E. W. de Menezes, and R. B. Ivanov, “Specific consumption of liquid biofuels in gasoline fuelled engines,” *Fuel*, vol. 87, no. 15–16, pp. 3362–3368, 2008, doi: 10.1016/j.fuel.2008.04.041.
- [34] R. Figaj, M. Szubel, E. Przenzak, and M. Filipowicz, “Feasibility of a small-scale hybrid dish/flat-plate solar collector system as a heat source for an absorption cooling unit,” *Appl. Therm. Eng.*, vol. 163, no. February, p. 114399, 2019, doi: 10.1016/j.applthermaleng.2019.114399.

- [35] J. Benajes *et al.*, “Analysis of the combustion process, pollutant emissions and efficiency of an innovative 2-stroke HSDI engine designed for automotive applications,” *Appl. Therm. Eng.*, vol. 58, no. 1–2, pp. 181–193, 2013, doi: 10.1016/j.applthermaleng.2013.03.050.



## APPENDIX A

The solar collector device that was built in Iraq at the University of Diyala - College of Engineering for the year 2015 was relied on. The readings and results of temperature and pressure used in this research were calculated on August 19, 2020, February 4, 2021, and March 3, 2021, using this solar collector.

### March 3, 2021

TIME	TEMPERATURE OF WATER (°C)	PRESSURE OF WATER (bar)
1:00 PM	30	0.5
1:20 PM	53	1.0
1:40 PM	65	1.7
2:00 PM	84	2.0
2:20 PM	92	2.6
2:40 PM	105	2.9
3:00 PM	117	3.2
3:20 PM	120	3.5

### February 4, 2021

TIME	TEMPERATURE OF WATER (°C)	PRESSURE OF WATER (bar)
1:00 PM	22	0.0
1:20 PM	38	0.6
1:40 PM	50	1.1
2:00 PM	61	2.0
2:20 PM	78	2.5
2:40 PM	85	2.9
3:00 PM	81	2.9
3:20 PM	75	2.7

**August 19, 2020**

TIME	TEMPERATURE OF WATER (°C)	PRESSURE OF WATER (bar)
1:00 PM	40	0.1
1:20 PM	65	1.7
1:40 PM	90	2.3
2:00 PM	110	2.8
2:20 PM	122	3.1
2:40 PM	130	3.4
3:00 PM	138	3.8
3:20 PM	143	4.0